Table of contents

1 Introduction

1.1 Click chemistry

Sharpless *et al.* presented, in 2001, a review in which they introduced the concept of "click chemistry".[1] In this review a "new way" of making chemicals, with a particular emphasis on drugs, is presented. Current drugs are often based on natural products that were first extracted from plants or other organisms and then with enormous effort were synthetically reproduced by chemists. Sharpless *et al.* propose to shift the focus away from the structure, which chemists focus on when they synthesize natural products, towards the function of molecules. Rather than making natural products with known biological activity and using these as templates for small modifications, it is proposed to make large libraries of compounds using (mainly) modular chemistry. After all, when looking for new and better drugs, it is the function that matters rather than the structure.

This approach mimics nature in that it involves making a great variety of different compounds starting from a relatively small number of building blocks *via* a set amount of reactions. These sets of reactions have been termed "click reactions" in which simple molecules with specific functionalities can be "clicked" to each other to form a large variety of compounds with relative ease that can subsequently be tested as potential drug candidates.[1]

For these "click reactions" Sharpless also looks to nature for inspiration. Nature makes use mainly of carbon-heteroatom bond formations, to make large functional molecules. Nature only uses carbon-carbon bond formation to form the initial building blocks that usually do not have more than six adjacent carbon bonds (with the exception of the aromatic amino acids). This also has the advantage that the formation of carbon-heteroatom bonds is usually energetically more favourable than that of carbon-carbon bonds.[1]

Sharpless *et al.* developed a set of rules to which a reaction must conform to qualify as a "click reaction". To be a "click reaction" a reaction needs to:

- be modular
- be applicable to a wide range of substrates
- produce high yields
- produce only inoffensive byproducts, that can be removed by non chromatographic methods
- be stereospecific, although not necessarily enantioselective

Ideally, the reaction conditions should be simple, involving no or benign solvents and the reaction itself should be insensitive to oxygen and water. To be able to obtain all of these characteristics these reactions need a high thermodynamic driving force, usually 20 kcal mol^{-1} or more. One could thus look at these reactions as being "spring loaded", so that as soon as the functional groups are in place the reaction can proceed easily and rapidly with high yields.[1]

Although several reactions exist that fulfill these requirements, the most popular one is the copper catalysed 1,3-dipolar cycloaddition of alkynes and azides. This reaction was discovered by the groups of K.B. Sharpless *et al.*[2] and Meldal *et al.*[3] (Scheme 2). The uncatalyzed version of this reaction was discovered by Huisgen[4] in 1964 (Scheme 1).

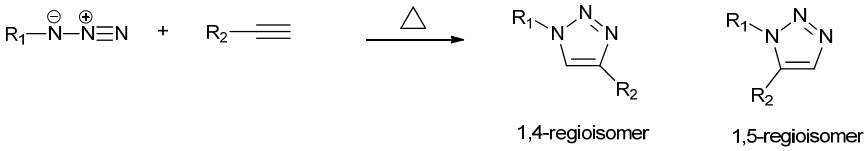

Scheme 1: Original Huisgen cycloadditon

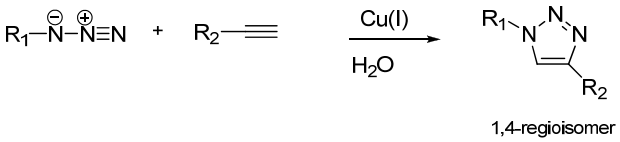

Scheme 2: Copper Catalyzed Huisgen cycloaddition

It was found that copper not only accelerates the reaction but also controls the regioselectivity since in the presence of copper, only the 1,4-isomer is formed. The copper catalyzed alkyne azide cycloaddition (CuAAC) has become very popular and is often considered as *the* 'click' reaction.

The CuAAC is a high yielding reaction (82-94%) for the wide variety of substrates demonstrated in the first papers in which it was published.[2, 3] It can be used for a wide variety of different R_1 and R_2 groups, although usually a terminal alkyne is required. The reaction proceeds in water, with or without co-solvent at room temperature and is relatively fast. The reaction is 100% atom efficient which means that there are no side products so the work up is usually simple. It can take place in a wide pH range which makes is suitable for biological compounds that require a specific pH. Furthermore the azide and alkyne functionalities are bioorthogonal, so theoretically, other functional groups present in a biological environment will not touch them. Finally the triazole product is biologically stable.

That the triazole is biolocally stable does not mean that it has no biological activity. The 1,2,3 triazole synthesized by the CuAAC is used in several drugs and inhibitors.[5] Another usages of the triazole is as an amide bond mimic. The distance with which two substituents are separated are similar for the triazole and an amide bond, furthermore the triazole has, just as an amide bond, a large dipole moment. [6]

Although the CuAAC is a rather fast reaction several groups have accelerated the reaction through the use of ligands. Fokin *et al.*[7, 8] discovered that TBTA (*tris*-(benzyltriazolylmethyl)amine) protects the copper in aerobic aqueous conditions. TBTA also realizes a tighter binding of the substrates, thereby stabilizing the oxidation state and lowering the activation barrier. Rodinov *et al.*[9] screened a large variety of ligands and showed that tris(2-benzimidazolylmethyl)amines have superior accelerating abilities. Histidine derivatives,[10] and phosphites[11] also show acceleration of the reaction. Pybox ligands do not only show acceleration but the chiral pybox ligands can also be used for a kinetic resolution of azides or alkynes.[12] Nolan *et al.*[13] showed that N-heterocyclic carbene ligands are able to accelerate the reaction and allow for the use of internal alkynes. Feringa *et al.*[14] have shown a significant rate acceleration with the easily synthesised MonoPhos ligand. MonoPhos accelerates the CuAAC to the extent that it is applicable to short lived isotopes.

1.1.1 Mechanism of the Cu Catalyzed Azide Alkyne Reaction

Finn *et al.*[15] have performed studies to get insight into the mechanism of the CuAAC. They performed kinetic studies which showed that with an excess of copper the experimental rate law was,

$$\text{rate} = k[\text{alkyne}]^{1.3\pm0.2}[\text{azide}]^{1\pm0.2}[\text{Cu}]^{0}$$

The rate law shows that when an excess of copper is present the reaction is first order in azide and 1.3 order in alkyne. That 1.3 order in alkyne could be explained if there are two pathways one involving, one alkyne and another involving two alkynes, occurring at the same time.

Based on the kinetics, they propose a mechanism in which the alkyne first forms a Cu-acetylide and later the azide coordinates to the metal, bringing both functional groups in close proximity. Subsequently the triazole ring is formed and released from the metal centre to form the product and regenerate the catalyst. It is still not clear whether there are multiple metal centers involved in the active catalyst.

Later Fokin *et al.*[16] used computational studies to gain more insight into the mechanism. Their calculations show that there is indeed a Cu-acetylide species formed. They first calculated the energy barriers of the uncatalyzed reaction for both the 1,4-isomer and the 1,5-isomer giving energy barriers of 25.7 and 26.0 kcal/mol respectively. This is in accordance with the 1:1 ratio found in non-copper catalyzed experiments. Subsequently they looked at the copper catalyzed version. The sequence begins with the coordination of the copper to the alkyne and then the formation of the Cu-acetylide species (Scheme 3).

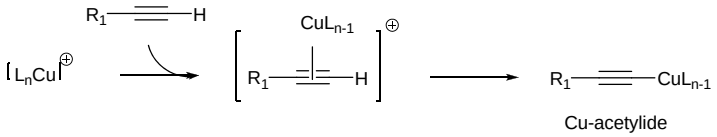

Scheme 3: Formation of Cu-acetylide

Activation of the triple bond via coordination, without deprotonation, gives an energy barrier of 27.8 kcal/mol which is even higher than that of the uncatalyzed reaction. Therefore it was concluded that the Cu-acetylide must be formed. When the alkyne replaces an acetonitrile ligand on the copper centre this step is slightly endothermic (0.6 kcal/mol) but when the replaced ligand is water the reaction becomes exothermic by 11.7 kcal/mol. This calculation explains the great rate acceleration observed when the reaction is performed in water. Calculations were then performed for the concerted reaction of the Cu-acetylide with the azide giving a barrier of 23.7 kcal/mol, which although lower, is not low enough to explain the enormous acceleration achieved by the use of copper.

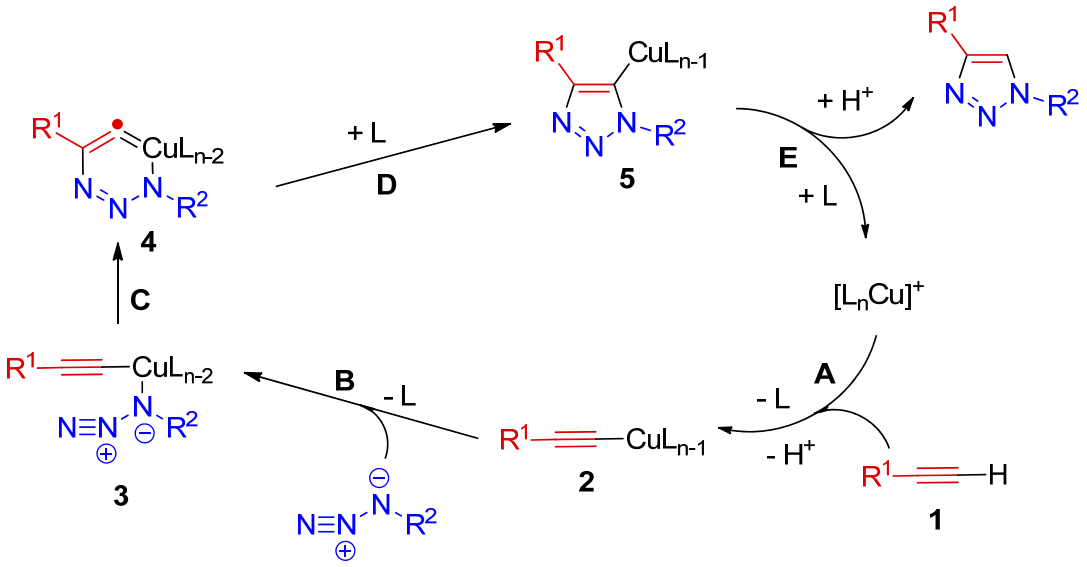

Scheme 4: Proposed mechanism of the CuAAC

Because of the high calculated energy barrier for a concerted mechanism this pathway was ruled out and coordination of the azide to the copper by replacement of one of the ligands is proposed as the next step. This energy barrier was set to 0 kcal/mol and yields compound 3 in Scheme 4. Then the formation of an unusual six-membered copper(III) metallacycle is proposed by attack of the distal azide nitrogen to the C2 carbon of the alkyne yielding compound 4. According to calculations this step is endothermic by respectively 8.2 or 12.6 kcal/mol for acetonitrile or water as the solvent. This gives a total energy barrier of 14.9 kcal/mol in acetonitrile and 18.7 kcal/mol in water. This is a lot lower than the barrier found for the uncatalyzed reaction.

These calculations give rise to the energy diagram shown in Figure 1. Most importantly this mechanism accounts for the enormous rate increase and it gives an explanation for the regioselectivity of the copper catalyzed reaction. Since they used for their calculations the azide as

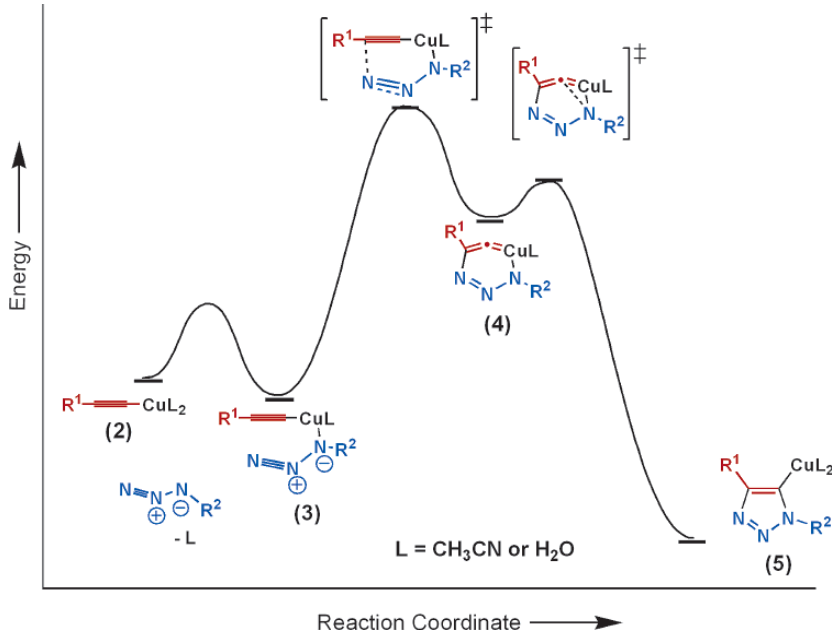

Figure 1: Energy diagram for the CuAAC

a dipole this would mean that other dipole alkyne reactions could also be catalyzed by copper. They show this experimentally using copper as a catalyst for the synthesis of various isoxazoles, the product of the cycloaddition of an alkyne and a hydroxylamine hydrochloride. Other dipoles like nitrones and nitrile oxides can also undergo [3+2] cycloadditions with alkynes[17].

Later more evidence for this proposed mechanism was found when Stroub *et al.,*[18] were able to trap the copper triazolide (compound 5 in Scheme 4), by using sterically demanding ligands in the absence of electrophiles.

1.1.2 Applications of the CuAAC "click reaction"

The CuAAC has been used throughout all fields of chemistry thanks to its high yields, its easily introduced functional groups and its orthogonality to many other reactions.[19] The *in vivo* stability of the triazole product makes the CuAAC a commonly used reaction for biological applications.

For instance Angelo *et al.*[6] use the triazole product from the CuAAC reaction to replace the amide bonds in peptides to create stable 'oligomers'. Conventional oligopeptides are biologically active and therefore interesting potential drug candidates. The problem is that the amide bonds in the peptides can be degraded *in vivo* through hydrolysis. By replacing the amide bonds with triazoles the 'triazole peptides' can not be so easily degraded and can be screened for biological activity. Two different tri and tetramers were synthesized in good yields (Scheme 5).

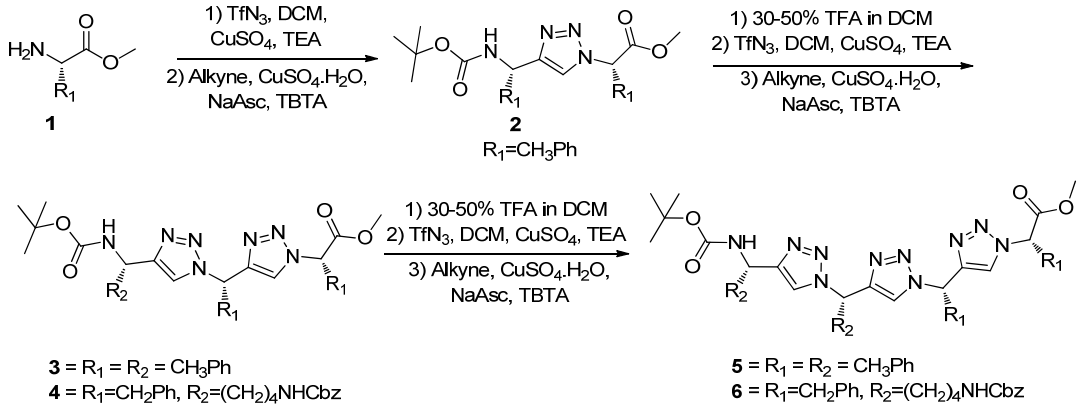

Scheme 5: Synthesis of trimers 3 and 4 and tetramers 5 and 6. Alkyne = BocNHCHR(1/2)CCH, TBTA = Trisbenzyltriazolamine

^{1}H NMR analysis of the synthesized tri and tetramers showed that these unnatural peptides have a zigzag conformation that mimics the β-strand structure of natural peptides. There are also other similarities between triazoles and amides, for instance both the triazole and amide bond have large dipoles, 5D and 3.5D respectively. Furthermore the sidechains of two neighboring amino 'acids' are separated by approximately the same distance in the triazole and amide case. This makes the triazole bond an interesting replacement for the amide bond.[6] Furthermore Tornøe *et al.*[3] showed that the CuAAC reaction can also be used on solid support making the synthesis of these unnatural peptides and other compounds even more convenient.

Another advantage of the orthogonality of the CuAAC is that it can be used in 'one-pot' procedures. Since NaN_3 is not sufficiently nucleophilic to undergo the 'click' reaction it will wait until it forms an organic azide and then click, therefore allowing it to be present in the reaction mixture with alkynes and copper without side reactions.[20, 21]

Because of the triazole stability and the orthogonality of the CuAAC towards other functional groups within a biological environment, the CuAAC is an ideal reaction to 'click' labels to biomolecules. For instance Duckworth *et al.* have introduced a CVIA tag in green fluorescent protein (GFP). Then they used Protein Farnesyl Transferase (PFTase) to specifically bind a diphosphate molecule with a 'click handle', in this case an azide (**7**, Scheme 6), to the cysteine in a CVIA tag. This method has now introduced selectively an azide at the end of the protein, which can be clicked to various (bio-)molecules. For instance *via* this procedure it is possible to 'click' fluorescent probes to proteins or (fluorescent) proteins to DNA (Scheme 6).[22, 23]

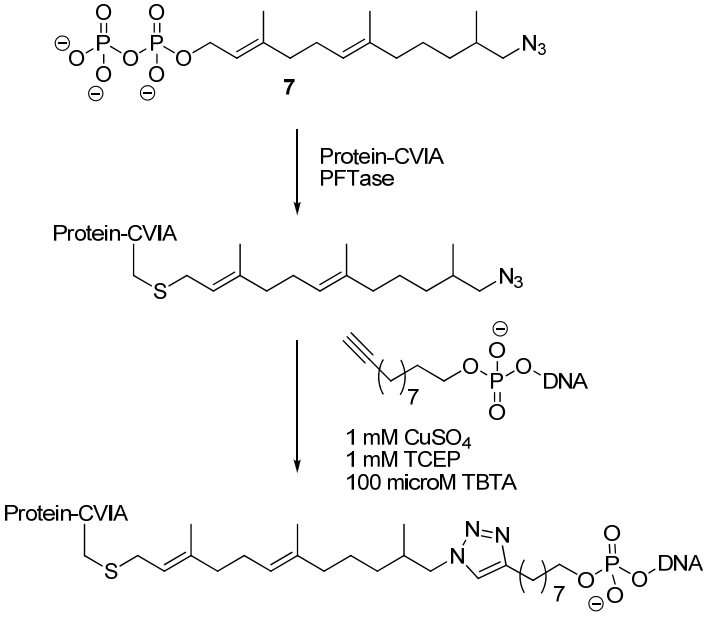

Scheme 6: PFTase-mediated labeling of target proteins with an azide molecule, and subsequent reaction with alkyne-modified DNA. TBTA=tris(benzyltriazolylmethyl)amine, TCEP=tris(2-carboxyethyl)phosphine.

Clark *et al.*[24] used an engineered *β*-1,4-galactosyltransferase enzyme (Y289L GalT) to specifically transfer an unnatural UDP substrate (1, Figure 2) onto an *o*-linked *β*-*N*-acetylglucosamine-modified protein. Since 1 contains an azide moiety, a fluorescent label (3, figure 2) or a biotin molecule (2, Figure 2) containing an alkyne which could be 'clicked' to the protein (Figure 2). Furthermore they show the specificity of the protein, so only in the presence of the enzyme, the UDP substrate 1 and biotin containing compound 2 a biotin labeled protein arises. The biotin labeled protein can then be visualized by a streptavidin-AlexaFluor 488 conjugate.

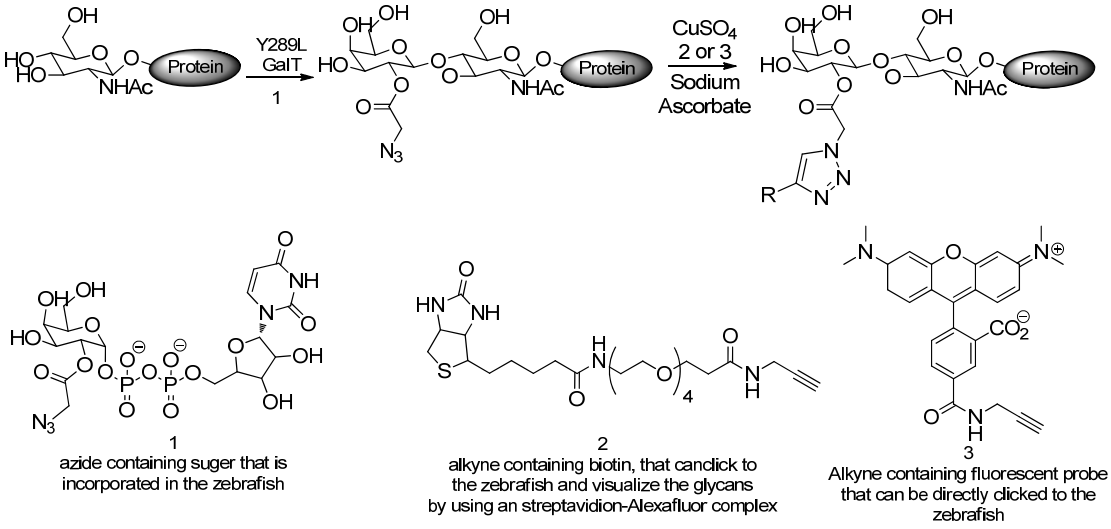

Figure 2: Synthesis of the fluorescent labeled protein (from ref. [24]).

Recently DNA has been labeled with the fluorescent dye Nile Red via the CuAAC. Beyer *et al.*[25] have synthesized an oligonucleotide with an 5-iodo-2'-deoxyuridine in the middle of the sequence. The halogen could be replaced *in situ* with an azide and subsequently coupled *via* the CuAAC to an alkyne functionalized Nile Red compound, yielding a fluorescent labeled DNA strand (DNA1, Figure 3). Comparison to a previously reported Sonogashira coupled DNA-Nile Red compound[26] shows that the triazole linked product has a slightly higher thermal stability, but that the optical data is similar. One of the advantages of this system is that halogenated precursors of every DNA base are commercially available, making it theoretically possible to introduce the 'click handle' at any desired place in the DNA sequence.

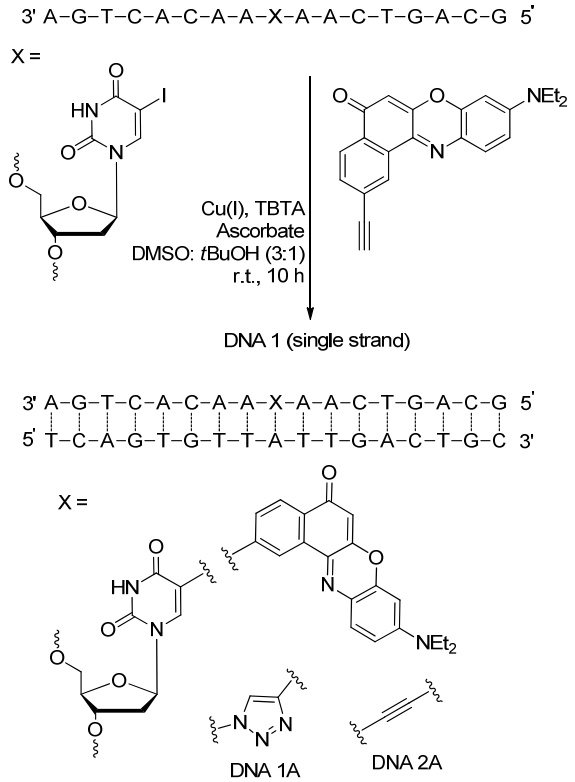

Figure 3: Synthesis of the triazole linked Nile Red DNA1 complex and corresponding DNA1A duplex. In comparison to the Sonogashira linked DNA2A (from ref.[25]).

1.1.3 Copper free Click chemistry

The bioorthogonality of the CuAAC and the fact that it proceeds readily in water at various pHs makes it suitable for biological applications. The main disadvantage is that copper is cytotoxic so this type of reaction cannot be performed *in vivo* and requires purification to eliminate traces of copper before labeled molecules can be monitored in biological systems. This is why chemists have put considerable effort into developing alkyne azide cycloadditions that proceed rapidly without copper, the Cu-free AAC.

To achieve Cu-free AACs an activated alkyne is needed. An activated alkyne can be obtained by introducing ring strain[27] and/ or electron withdrawing groups. Bertozzi *et al.* use a strained cyclooctyne[28] and showed that the introduction of fluorine as an electron withdrawing group (EWG) adjacent to the acetylene enhances the rate of the cycloaddition compared to other functionalities[29]. Another advantage of fluorine as an EWG, is that the fluorine is more stable in biological systems.

For the imaging of glycan trafficking in zebra fish Bertozzi *et al.* [30, 31] synthesized **8** following the procedure shown in scheme 7. Compound **8** has an activated alkyne that is able to react with simple azides with a 2nd order rate constant of 7.6 x 10^{-2} M^{-1} s^{-1}. The acid group of **8** was used to attach a fluorescent label, Alexa fluor 488 or 568, or biotin. Developing zebrafish embryos were treated with unnatural sugars containing an azide functionality. The embryo's build these sugars into their cell surface glycans. When the zebrafish embryos are then exposed to the labeled compound **8** the free azides will react with the activated alkyne in a Cu-free AAC thereby attaching a fluorescent label to the cell surface glycans.[30, 31]

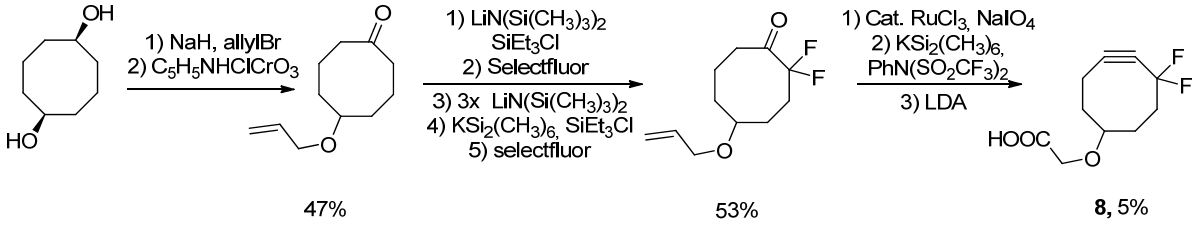

Scheme 7: Synthesis of activated alkyne 8.

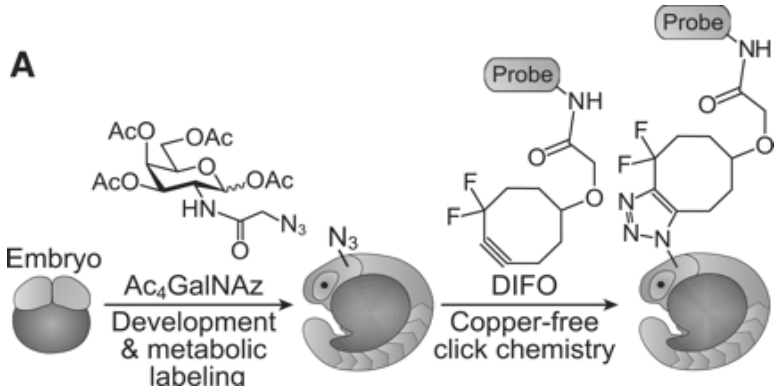

Figure 4: Schematic representation of the metabolic labeling for the noninvasive imaging of glycans (from ref. [31]).

Recently Bertozzi *et al.* also showed the power of this procedure by labeling azidosugars in live mice[32]. Since not all fluorinated cyclooctyne probes were easily dissolved in water DIMAC (**9**)

was synthesized from 6-bromoglucopyranoside. DIMAC solved the solvation problem but had as a disadvantage that it was approximately 40 times slower [33] than fluorinated compound **8**.[34]

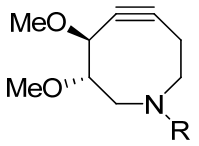

9, DIMAC

Since the publication of the strained cyclooctyne for Cu-free AAC, the technique has been used in various fields of chemistry. It has been used to create a hydrogel that can be formed in the presence of cells thus encapsulating the cells in the gel[35] and for the formation of poly(amide)-based dendrons and dendrimers with no copper contamination.[36] Schultz *et al.* recently showed a high yielding three step synthesis to the strained cyclooctyne **10** (Scheme 8). They used the free acid of compound **10** to attach a biotin molecule and subsequently used the Cu-free AAC to attach the biotin label to a azide-modified DOTA molecule.[37, 38]

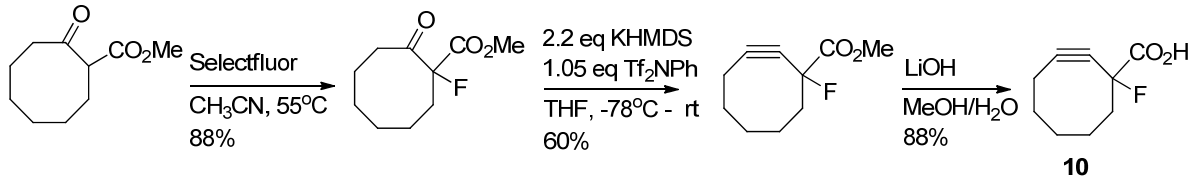

10

Scheme 8: Synthesis of 10.

Boons *et al.* introduced more ring strain to their system by adding phenyl rings adjacent to the cyclooctyne functionality resulting in compound **11** that has a 2nd order rate constant of 2.3 M^{-1} s^{-1} in water/acetonitrile (1:4). By attaching a biotin molecule to the free alcohol and 'clicking' the cyclooctyne-biotin construct to the azido containing cell surface of Chinese hamster ovary cells it was possible to visualize the cell surface of the cell with an avidin-Alexa Fluor 488 complex.[39] Van Hest *et al.* use two molecules of compound **11** attached to both ends of a polyethylene glycol (PEG) linker as crosslinker for a copper free click coating.[40]

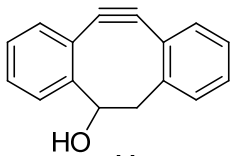

11

A comparable aza-dibenzocyclooctyne **12** was synthesised by van Debets *et al.*[41] Advantages of **12** are that it is easier to synthesize, the label is attached via an amide bond instead of the weaker ether bond and the compound is less hydrophobic making it more soluble in water. Furthermore the second order rate constant is 0.31 M^{-1} s^{-1}, almost as fast as the click reaction with compound **11**.

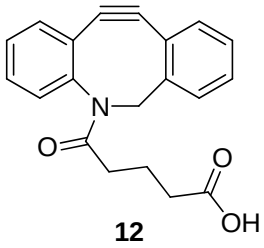

12

The introduction of phenyl rings to increase the reactivity of cyclooctynes has also inspired Bertozzi *et al.* to combine the extra ring strain with the electron withdrawing effects of the fluorine substituents resulting in compound **13** with a 2nd order rate constant of 0.22M^{-1} s^{-1}.[42] Unfortunately compound **13** was unstable forming di- and trimers, though it was shown that *β*-cyclodextrin was able to stabilize cyclooctyne **14**, so that no formation of the di- and trimers occurred. Dibenzylated cyclooctyne **14** showed a 2nd order rate constant of 0.96 M^{-1} s^{-1} and proved to be more sensitive in cell labeling experiments then the previously synthesized cyclooctynes.[33]

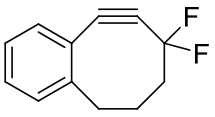

13

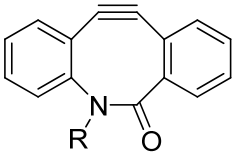

14

Another highly strained and therefore highly reactive alkyne is benzyne. A mild way to form benzyne is by fluoride-induced ortho-elimination of o-(trimethylsilyl)phenyl triflate.[43] Feringa *et al.* used this *in situ* formation of benzyne and subsequently 'clicked' the benzyne to benzyl azide, yielding product **15** in good yields (Scheme 9).[44]

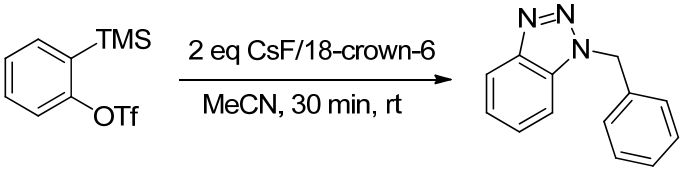

15, 77%

Scheme 9*: In situ* formation of benzyne followed by Cu-free AAC yielding compound 15.

In three cases non cyclooctyne alkynes are used for Cu-free AAC. Clark *et al.*[45] use compound **16** as crosslinker for azide containing polymers. At 37°C hydrogels are formed within 1-8 days. Ni *et al.*[46] were able to polymerize imine **17** in the absence of copper under ambient conditions in 14 days. Li et al.[47] provide a faster system, which uses internal or external alkynes with acid or ether functionalities as EWG. When the activated alkynes are stirred with ethyl 5-azidovalerate in water they yield the triazoles in 67-94% within 6-12h.

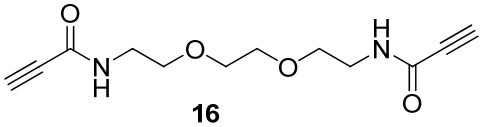

16

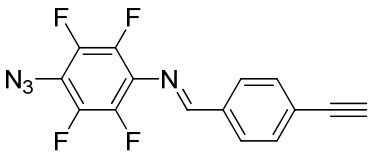

17

1.2 Positron Emission Tomography

Positron Emission Tomography (PET) is a nuclear medicine imaging technology that is able to provide 3D images of the human body. It is based on radioactive positron emitting atoms.[48] Radioactive compounds undergo decay, and when this happens they emit a positron or an electron, called β^+ or β^- decay, respectively. When an emitted positron encounters an electron, that combination will result in the annihilation of both particles under the emission of two photons. During this reaction mass is converted into energy following $E=mc^2$. The emitted photons have an energy of 511 –keV and move in opposite directions.[49] During a PET scan a subject is injected with a radioactive sample. When the sample decays the emitted photons are detected and subsequently it can be subsequently determined where high concentrations of the radioactive tracer were present in the subject (Figure 5).

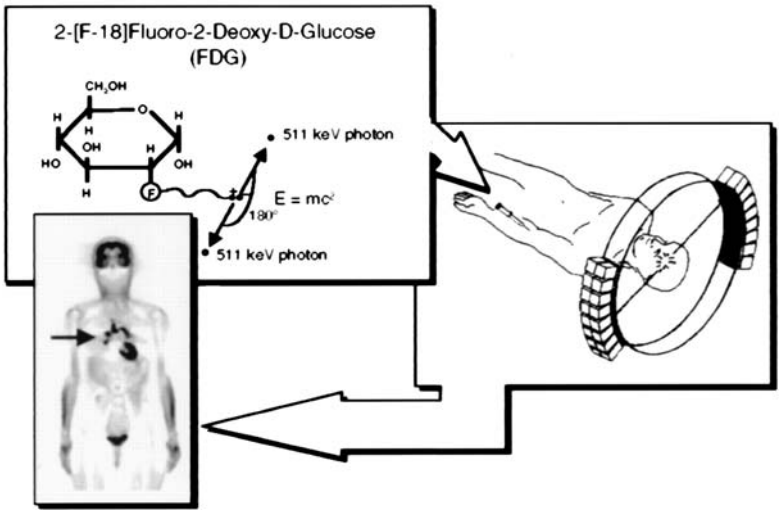

Figure 5: Principles of PET, left the readily used FDG molecule with ^{18}F emitting two photons, which can be detected by the PET apparatus (right) leading to a 3D image of the subject (from ref.[49]).

There are several radiotracers that can be used for PET from the 2nd period elements; ^{15}O, ^{13}N, ^{11}C and ^{18}F are all positron emitters. Of these, ^{18}F is most often used because of its long half life, 110 min.[50] A commonly used compound for PET is the glucose analogue 2-[F-18]Fluoro-2-Deoxy-D-Glucose (FDG). FDG can, just as glucose, be phosphorylated by hexokinase, the difference with glucose is that the phosphorylated product of FDG, FDG-6-PO_4 is not significantly used in subsequent reactions in the body on the PET timescale. The FDG-6-PO_4 will remain in the cell where it is phosphorylated thereby giving a measure of the extent to which glucose is phosphorylated in that cell.[49]

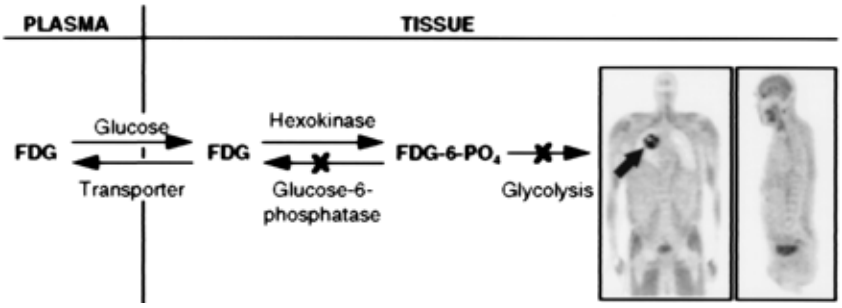

Figure 6: Phosphorylation of FDG and resulting PET images.[49]

Diseases are biological processes that often require more energy, as in the form of glucose, than normal processes especially in cases like that of cancer where the disease is fast growing. The injected FDG will be phosphorylated in higher amounts in the cancerous areas than in other areas giving a good high resolution 3D image of the disease (Figure 6).[49]

1.2.1 Click chemistry for PET

The radioactive ^{18}F is usually directly introduced into the compound of interest. Often this is achieved by an S_N2 reaction with a $^{18}F^-$ anion acting as the nucleophile.[50] However to make the fluorine anion highly reactive it needs to be dried to remove all solvated water molecules which makes the anion less reactive. In the drying process a base is added, meaning that the to be labeled compound must be stable in the presence of base. Since this significantly limits the scope of this labeling methodology significantly other methods have been developed.[50]

A quick way to introduce ^{18}F was described by Kim *et al.*.[51] They use protic solvents such as tertiary alcohols to accelerate the introduction of $^{18}F^-$ in compounds containing a mesylate or tosylate. At a 100 to 120 °C in 10 to 20 min they obtain the desired products in good radio chemical yield (RCY) (Table 1). Radio chemical yield is the yield based on the radioactivity of the product divided by the radio activity of the starting material. Because the radioactivity decays not only the amount of product formed but also the reaction time plays an important role in obtaining a high RCY.

Entry	*Compound*	*[^{18}F]fluorination temp. (°C)*	*Time (min)*	*Precursor (mg)*	*RCY (%)*	*Product*
1	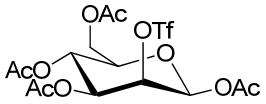	100	10	20	85.4 ± 7.8 (n = 10)	[^{18}F]FDG
2	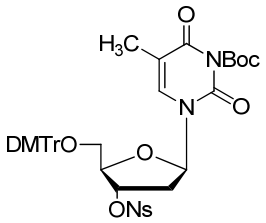	120	10	20	65.5 ± 5.4 (n = 10)	[^{18}F]FLT
	Method in lit.[52]	110	7.5	20	15.0 ± 5.4 (n = 3)	[^{18}F]FLT
3	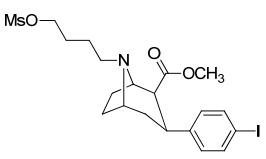	100	20	4	35.8 ± 5.2 (n = 14)	[^{18}F]FP-CIT
	Method in lit.[53]	90	10	10	Only 1%	[^{18}F]FP-CIT

Entry	*Compound*	*[18F]fluorination temp. (°C)*	*Time (min)*	*Precursor (mg)*	*RCY (%)*	*Product*
4	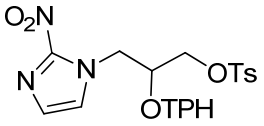	120	15	10	69.6 ± 1.8 (n = 10)	[18F]FMISO
	Method in lit.[54]	105	6	10	15.0 ± 5.4 (n = 3)	[18F]FMISO

Table 1: Results of Kim *et al.* for the introduction of ^{18}F in various compounds.[51]

Because of the rapidly decaying radioisotopes it is very important in PET to be able to introduce the radioactive labels in a quick way with no or harmless byproducts since standard purification methods often take too much time. This is where 'click' chemistry comes in. Marik *et al.* were the first to publish the use of the CuAAC to readily 'click' a radiolabel to a small peptide (Scheme 10). When n = 2 the reaction showed high yields, >97% and good purity >81%, highlighting the usefulness of the CuAAC for PET labeling.[55]

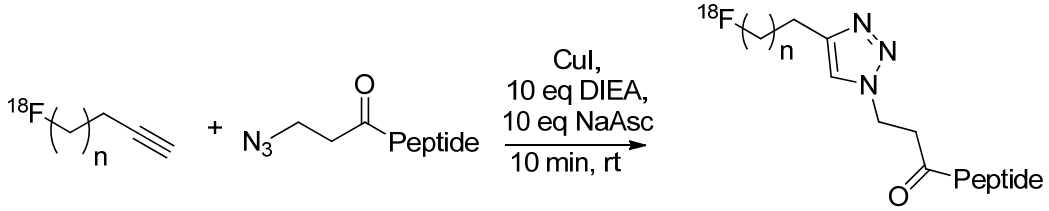

Scheme 10: CuAAC for the labeling of small peptides with a ^{18}F-radioactive isotope.[55]

By combining the ^{18}F introduction of Kim *et al.* and the 'click' for PET concept of Marink *et al.* Sirion *et al.*[56] showed a quick one-pot reaction, with no need for interim purification, to attach a PET label to biomolecules. Glaser *et al.* reversed the azide and alkyne containing compounds by synthesising an azide containing ^{18}F compound that they subsequently reacted in good yields, with commercially available alkynes.[57]

Li *et al.*[58] used the CuAAC to connect a ^{18}F containing alkyne to a cyclic RGD (Arganine-Glycine-Aspartic Acid) peptide and showed the distribution of the peptide with microPET, a small PET apparatus for experiments with mice. Hausner *et al.* labeled the peptide A20FMDV2 with a ^{18}F containing compound via the formation of an amide bond and via the CuAAC (Scheme 11). The 'clicked' product could be obtained faster, resulting in a higher RCY, but required more peptide precursor.[59] They also found, during the *in vivo* animal studies, that the radioactive label has a significant effect on the properties of the peptide. For this reason alone it would be preferable to have several techniques used for labeling to investigate the most favorable labeling procedure for each compound.

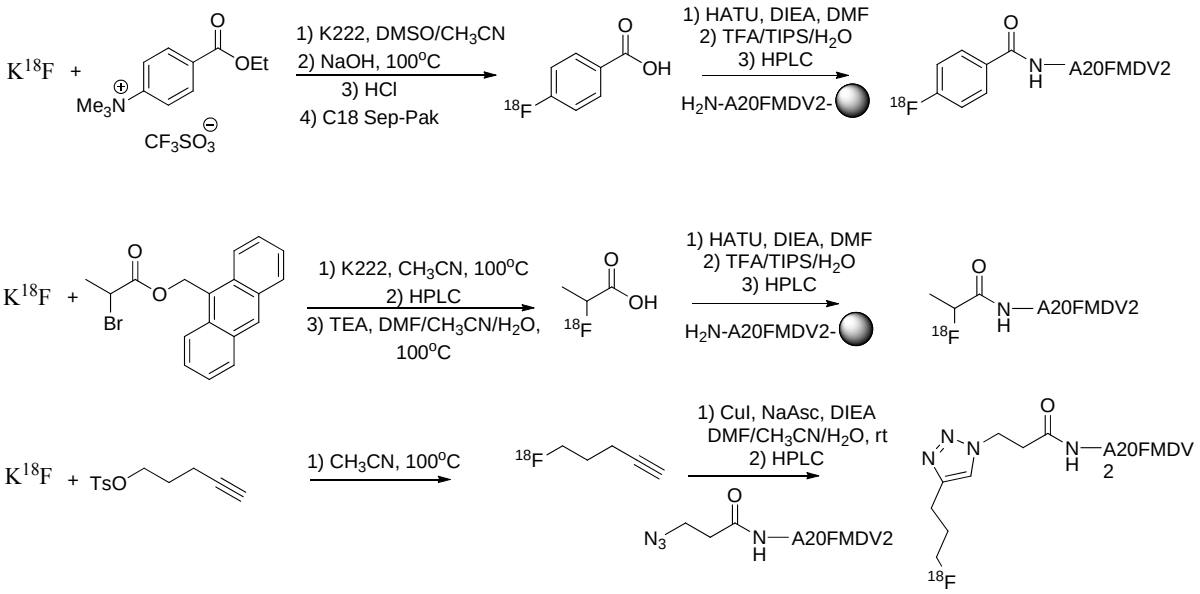

Scheme 11: Labeling of peptide A20FMDV2 *via* an amide bond and *via* 'click' chemistry.

1.3 Fluorescence

Fluorescence is one of the photochemical processes that can take place when light interacts with matter. The electrons of a molecule will usually reside in the lowest available energy state, called the ground state (S_0). The Jablonski diagram in figure 7, shows the ground state (S_0), the singlet excited state (S_1) and the triplet excited state (T_1), each of these energy states is represented as a Morse potential. In the Jablonski diagram the vertical axis represents the potential energy and the horizontal axis the structural properties of the energy states. So S_1 and T_1 are higher in energy than the S_0 ground state, furthermore the Jablonski diagram shows that S_0 and S_1, which have a similar place along the horizontal axis, are similar in structure, while T_1 has a different structure.[60]

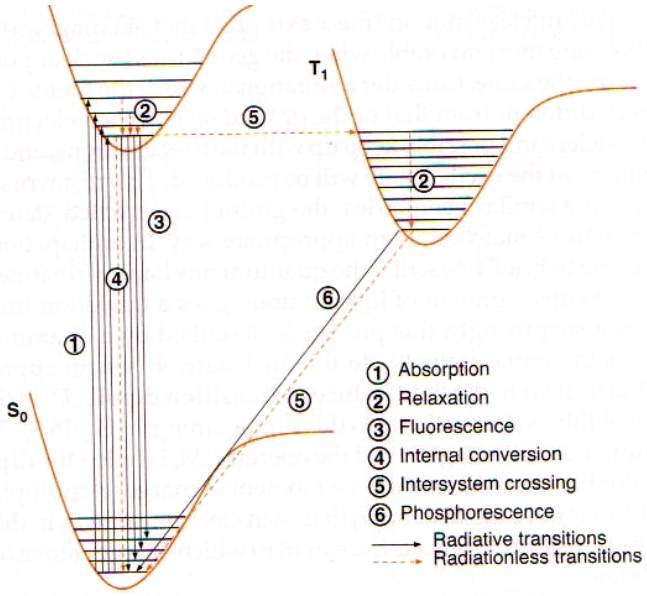

Figure 7: Jablonski diagram [60]

The horizontal lines in the Morse potential diagrams represent the vibrational energy levels of the energy states. An electron that is in the ground state can be excited to a higher energy state, for instance S_1. This energy can be applied in the form of light (photons) of the right wavelength

(energy). The phenomenon in which photons excite electrons to a higher energy state is called absorption (1 in figure 7). The electrons can be excited to several vibrational levels of the excited state. When the electron is excited to one of the higher vibrational levels of the excited state the electron will immediately, in +/- 1 ps, relax to the lowest vibrational level of the excited state (2 figure 7).[60]

The still excited electron will want to fall back to it's initial, lower energy ground state which takes +/- 1-10 ns. For the return to the ground state the electron must lose it's excess energy, for instance through the emission of a photon (light). This process is called fluorescence (3 figure 7). Again the electron can fall back to the several vibrational levels of the ground state. Because the relaxation is so much quicker than the fluorescence, the fluorescence will always occur from the lowest vibrational level of S_1. This has the consequence that the emitted light is always of lower energy, and thus of higher wavelength, than the excitation energy.[60, 61]

An important measure for the amount of fluorescence is the quantum yield (Φ). This measure is given by dividing the total amount of absorbed photons by the amount of emitted photons. So effectively the quantum yield is a measure for the efficiency of the fluorescence, in which a quantum yield of 1 implies a 100% efficiency, of a specific fluorophore.[60, 61]

1.3.1 Fluorescence imaging

Fluorescence imaging is one of the most basic and widely used tools for biological imaging. By attaching a fluorophore to a biomolecule the biomolecule can be visualized by excitation of the attached fluorophore and detection of the emitted fluorescence. This imaging technique has the advantage that it is highly specific and that it has a good signal to noise ratio, due to the abscence of background fluorescence,. Another advantage is that the emitted fluorencense is detected at a different wavelength than that at which it is excited resulting in little background noise.[61, 62]

To initiate fluorescence the sample needs to be irradiated at the correct wavelength. There are three ways of exciting the fluorophore present in the sample. The first is called wide-field, and uses a lamp that produces 'white light', light in the range of the visible spectrum, and has high intensities at wavelengths characteristic for the lamp used. The other options are to irradiate the sample with a laser either at the excitation wavelength or at a lower wavelength so that two photons are needed to excite the fluorophore. Two-photon laser scanning fluorescence microscopy has the advantage that a small area can be radiated resulting in less photobleaching (loss of the ability of a sample to fluoresce due to irradiation of the sample)[61, 63]

There are various fluorescence imaging techniques using either one or more fluorophores depending on the process under investigation, all of which provide different information about the labeled molecule(s). Below these techniques are described shortly.

- ***Immunofluorescence[61]:*** The most widely used fluorescent imaging technique. Simply put it consists of labeling the molecule of interest with a fluorophore, exciting the fluorophore and detecting the emitted light. In this way the distribution can be visualized both qualitatively and quantitatively. Most examples shown in sections 1.1.2 and 1.1.3 are following this technique.

- ***Fluorescence In Situ Hybridisation (FISH)***[61]: Similar to immunofluorescence but is used for the labeling of DNA and RNA. By labeling the complementary DNA or RNA strand, the DNA/ RNA strand of interest can be visualized.
- ***Quantitative Colocalization Analysis***[61]***:*** This technique uses two fluorophores which emit light of different complementary wavelengths. For instance by labeling one protein with a red dye and another, relatively similar protein, with a green dye it can be visualized whether these similar proteins reside at the same place in the cell. When they reside close to each other the light emitted will appear yellow.
- ***Fluorescence Ratio Imaging (RI)***[61, 64]***:*** Uses a fluorophore that has the ability to emit light of two different wavelengths depending on the environment. For instance there are fluorophores that change the wavelength at which they emit upon ion binding. This way the ratio of bound and unbound fluorophore can be determined, which gives an indication of the ion concentration.
- ***Fluorescence Resonance Energy Transfer (FRET)***[60, 61]***:*** FRET is a phenomenon that can take place when two fluorophores are in close proximity. It occurs when the potential energy of the donor fluorophore is large enough to excite the acceptor fluorophore. Since this transfer of energy can only take place when the donor-acceptor couple are in a radius of approximately 1-10 nm of each other, labeling a protein with a donor and another protein with an acceptor fluorophore allows the protein-protein interactions of these proteins to be studied.
- ***Fluorescence Lifetime Imaging (FLIM)***[61]***:*** During FLIM the lifetime of the fluorophore is followed. The lifetime is the time the excited electron resides in the excited state. The changes thus give a measure for the occurrence of other processes by which the excited electron can lose its energy. Examples of such processes are photobleaching, internal conversion and FRET.
- ***Fluorescence Recovery After Photobleacing (FRAP)***[61]***:*** A technique that can be used to determine the mobility of the labeled molecules. It starts by photobleaching a small area and subsequently following the time it takes for the labeled molecules to restore the fluorescence in that area. This gives an indication of how mobile the labeled molecules are.
- ***Total Internal Reflectance Fluorescence Microscopy(TIRFM)***[61]***:*** When a light beam is shone at just the right angle at the sample the light will be completely internally reflected. This results in less photobleaching and less background noise since only a small shallow area is irradiated. The disadvantage is that only processes close to the cell membrane can be visualized since the light does not penetrate far into the sample.
- ***Fluorescence Correlation Spectroscopy (FCS)***[61]***:*** A very sensitive technique that uses the small changes and movements of fluorescent labeled molecules as a signal. Thereby yielding information about the location, accumulation and mobility of the labeled molecules.

1.4 Dual imaging techniques

To achieve better understanding of the human body and the diseases that strike it, several imaging techniques have been developed over the years. Two of these, PET and fluorescence have already been discussed in previous paragraphs. Other imaging techniques are single photon emission computed tomography (SPECT), magnetic resonance imaging (MRI), magnetic resonance spectroscopy (MRS) and ultrasonography (US).[65, 66]

All of these techniques have their own advantages and disadvantages. PET for instance has a high sensitivity, thus only small amounts of radiotracer are necessary. On the other hand PET has the disadvantage that is has a low resolution. MRI and CT provide high resolution 3D images but suffer from low sensitivity. Optical (fluorescence) imaging has generally a good sensitivity but can only help visualize processes close to the surface because of the limited light penetration. To achieve better images, methods to combine imaging techniques resulting in dual imaging have been developed.[65, 66]

There are two ways to combine multiple imaging techniques. One is to combine the instruments and the other is to combine the two functions needed for the two imaging techniques in one probe. This last one has the advantage that both imaging techniques are then imaging the same molecules and thus the same biological process. Herein lies the great challenge for synthetic chemists to develop new probes that are, preferably, small, so that they interfere as little as possible with the biological function, while containing two imaging functionalities.[66]

1.4.1 Combining PET and fluorescence imaging

PET and fluorescence imaging are a promising combination for dual imaging technology. They both have high sensitivity resulting in a PET-fluorescence probe that can be present in low quantities while still allowing good images from both techniques. The deep tissue imaging of PET and the longer lasting imaging of fluorescence allows for the possibility for the localization of a disease with PET and then the visual guide of fluorescence during surgery all with one probe. Especially when short lived isotopes such as ^{11}C and ^{18}F are used, the fluorescent label gives information about the distribution and metabolic breakdown of the labeled drug or tracer.[65, 66]

Thus far the synthesis of dual modality probes has mainly focused on the use of long lived isotopes such as ^{86}Y, ^{64}Cu, ^{68}Ga and ^{124}I. Short lived isotopes present an extra challenge to the synthesis since the introduction and subsequent purification of the isotope has to occur within a small time frame, preferably less than an hour. The disadvantage of the long lived isotopes are that the subject is exposed to the radioactivity for a longer period of time.[65, 66]

Kimura *et al.*[67] have published an example of a PET/ fluorescence dual modality probe. It is known that cancer cells contain differential or overexpression of proteins for the formation of new blood vessels to enable tumor growth. The integrin receptor proteins $\alpha_v\beta_3$ and $\alpha_v\beta_5$, which play a role in signaling and cell attachment, are examples of these overexpressed proteins. The engineered knottin peptide 2.5D is a known binder for the integrin receptors $\alpha_v\beta_3$ and $\alpha_v\beta_5$. [68]Kimura *et al.* started from this peptide and were able to attach a DOTA fragment to bind the long lived radio isotope ^{64}Cu and the near infra red fluorescence fluorophore Cy5.5 resulting in compound **18** (scheme 12). When compound **18** was injected in tumor containing mice both fluorescence imaging and PET gave a good indication of where the tumor was present. This shows

that the addition of the two imaging functionalities did not destroy the binding affinity of the peptide.

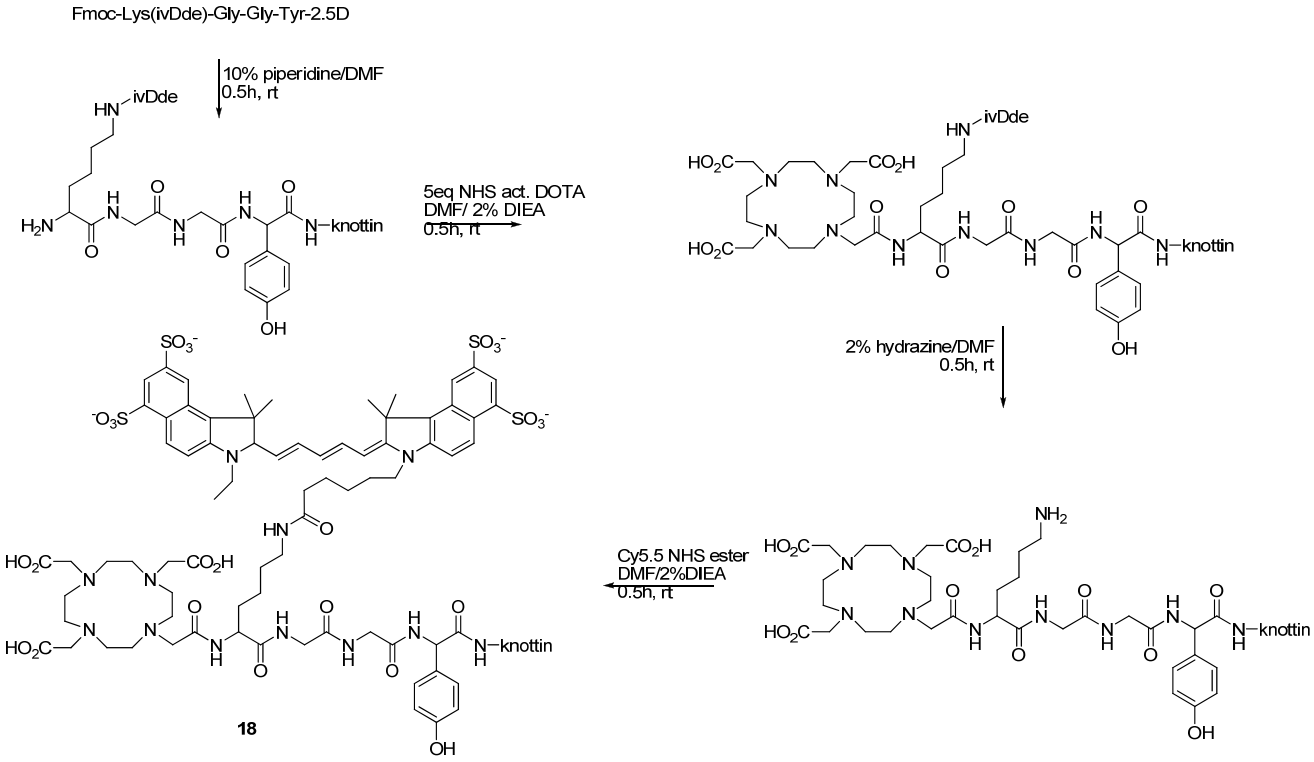

Scheme 12: Synthesis of the dual modality probe 18, for PET and NIRF imaging.

2 Goal of the research

The goal of this research consists of two parts. The first is to employ the Cu-free AAC for the synthesis of PET tracers. As indicated in the introduction the CuAAC is already employed for this purpose. By using the Cu-free AAC, with one of the highly activated cyclooctyne systems, the advantages of 'click' chemistry, namely the short reaction times, the mild conditions and the bioorthogonality will still apply. Another advantage will be added, since the copper is no longer present during the reaction it does not have to be removed afterwards. Furthermore is opens the possibility for reactions to occur *in vivo*. With the high yields and the lack of side products hopefully no purification will be needed. In this way precious time, in which the PET label decays, is saved.

The other part of the project will focus upon the synthesis of a dual modality probe for PET and fluorescence imaging. It is clear that by combining two imaging techniques more information can be obtained. So far the focus has been on long lived isotopes which have been used for the combination of PET with fluorescence imaging, primarily because the short lived isotopes do not provide a long enough time frame for the synthesis of such complex dual modality probes. By synthesizing an already fluorescent labeled biomolecule with a 'click handle' the radioactive tracer ^{18}F could be introduced *via* the fast and bioorthogonal 'click' reaction.

3 Synthesis of a strained cyclooctyne for Cu-free AAC

To use Cu-free AAC for PET a highly reactive alkyne is needed to achieve the short reaction times necessary for the work with short lived radioactive isotopes. For this reason it was decided to synthesize compound **11** as published by Boons *et al.* This compound was chosen because it has a high 2nd order rate constant and the reported synthesis consists of five high yielding steps.

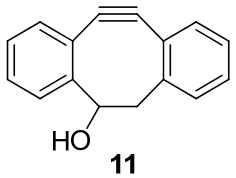

11

3.1 Synthesis of 3-hydroxy-7,8-didehydro-1,2:1,5-dibenzocyclooctene.

The first step of the synthesis entails the formation of ether **26**, which was first published by Jung *et al.*[69]. Phenylaldehyde was stirred with 1.2 equivalents of trimethylsilyliodide (TMSI) under a nitrogen atmosphere at 5°C for 7 days. In the proposed mechanism (scheme 13) the phenylaldehyde reacts with TMSI to give the TMS protected compound **20**. Subsequently the TMS protected oxygen attacks another carbon with iodide acting as a leaving group resulting in the silylated oxonium iodide **21**. Upon loss of trimethylsilyliodide the acetal **22** can be formed. There are two proposed pathways that can be taken to form iodo ether **25**. Pathway A goes *via* a Friedel-Crafts cyclization with iodide acting as the leaving group. Subsequent loss of a proton to restore the aromaticity yields acetal **23**. Attack of the iodide ion of either HI or TMSI yields the iodo ether **24**. In the other pathway, B, the Friedel-Crafts cyclization and attack of the iodide anion are reversed. First attack of the iodide ion occurs yielding diiodo ether **23**, which forms iodo ether **25** upon Friedel-Crafts type cyclization.

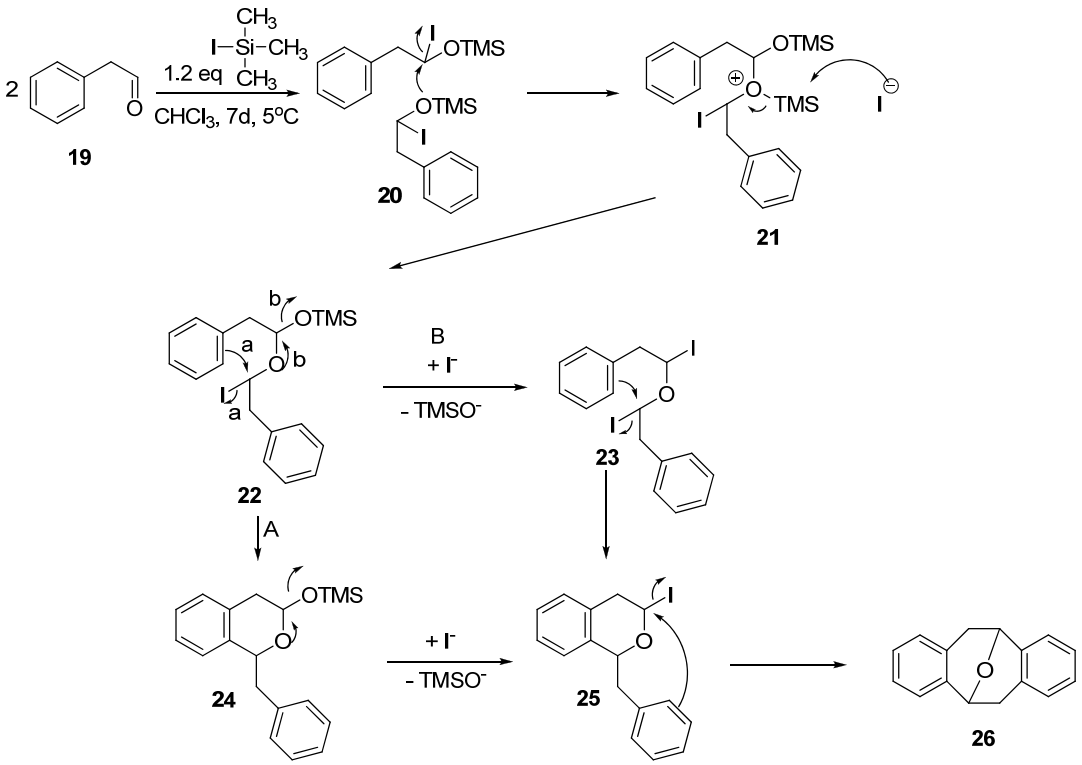

Scheme 13: Proposed mechanism of the formation of ether 26.

Another potential reaction under these conditions would have been the attack by one aldehyde molecule on the favorable *para* position of the aromatic ring of another phenylaldehyde molecule, scheme 14. However no *para* substituted byproducts like **27** are observed and this is a strong indication that the mechanism follows a pathway that takes place *via* complexation of the two phenylaldehyde molecules prior to the Friedel-Crafts reaction. The proposed initial formation of acetal **22** prior to the Friedel-Crafts reaction only allows *ortho* substitution.

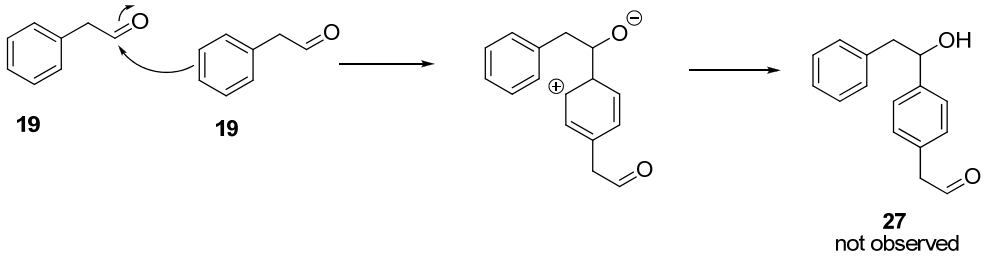

Scheme 14: Friedel-Crafts reaction of phenylaldehyde on the *para* position.

Jung *et al.* supported their mechanism by the reaction of 2-phenyl-ethyl trimethylsilyl ether **28** with trimethylsilyliodo adduct of acetaldehyde **29**. This reaction indeed yielded the *ortho* substituted ether **33**, presumably *via* the same initial complexation (**30**) and subsequent loss of TMSI and finally the Friedel-Crafts cyclization (**32** Scheme 15).

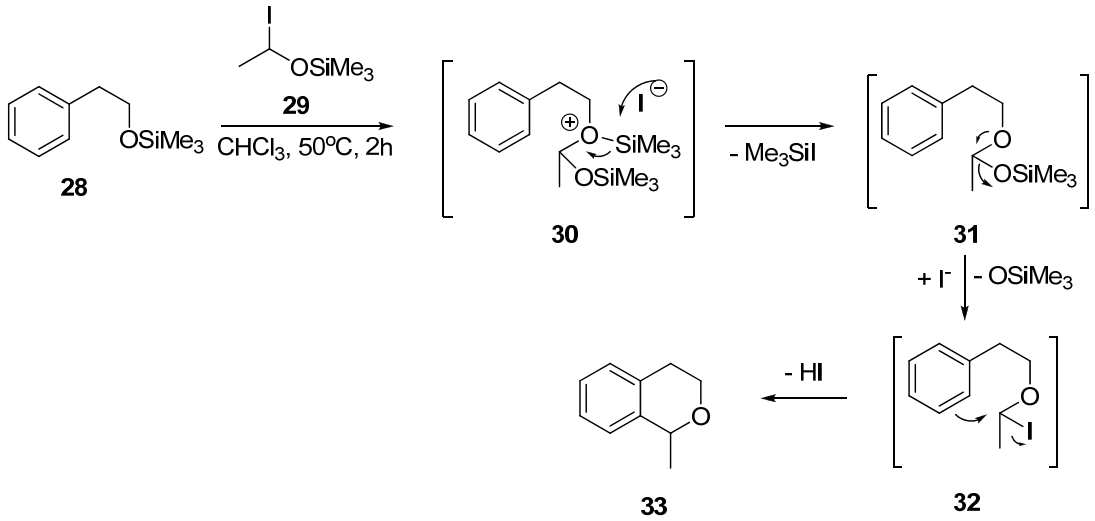

Scheme 15: Support for the proposed mechanism in scheme 13.

Jung *et al.* report a 50% yield of ether **26**. Unfortunately upon repetition of the procedure a yield of 33% at most was obtained. It was hypothesized that the difference in yield might be due to the use of commercially available TMSI, as opposed to the freshly distilled TMSI used in the publication. Synthesis of TMSI was attempted by stirring LiI and TMSCl at r.t. in $CHCl_3$ for 4 h[70]. Due to the high reactivity of TMSI towards moisture in the air, TMSOH was formed during purification. It was then decided to form the TMSI *in situ* during the reaction (Scheme 16) and the resulting crude ^1H NMR gave a better product to side product ratio than the original synthesis.

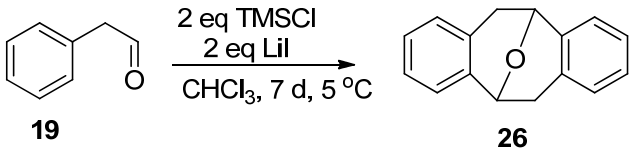

Scheme 16: Formation of ether 26 with *in situ* formation of TMSI.

The second step of the synthesis is the formation of alkene **34**, by treating ether **26** with n-BuLi (scheme 17).[71] Jung *et al.* first tried to open the methoxy substituted ether **35** in their synthesis of isopavine under acidic conditions, but the ether proved stable to all acids tested. When a model was built, one of the vicinal benzylic carbon-hydrogen bonds proved to be precisely anti-coplanar to the carbon-oxygen bond of the ether, leading the way for E2 elimination. Indeed treatment with the strong base n-BuLi yielded the ring opened product. They found that use of excess base (2 equivalents) gave higher yields of the alcohol. They ascribed this to the destruction of base by deprotonation of aromatic protons.

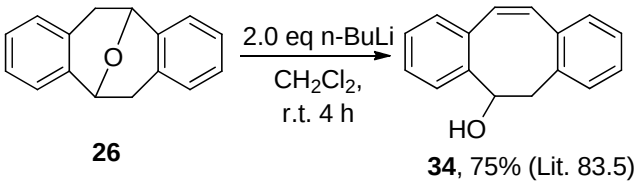

Scheme 17: Second step of the cyclooctyne 11 synthesis.

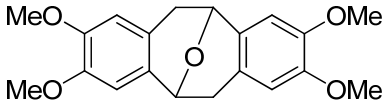

35

The next step in the synthesis is the protection of the alcohol as *tert*-butyl-di-methyl-silylether **36** prior to the bromination of the double bond (Scheme 18). The TBDMS-protecting group falls off during the bromination. The hydroxyl group was protected because Ning *et al.*[39] report a low yield for the bromination in the absence of the protecting group.

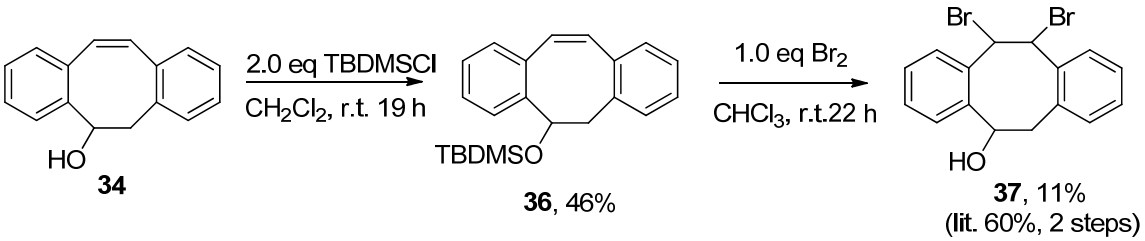

Scheme 18: Protection and subsequent bromination affording compound 37.

Because we found low yields for the protection with TBDMSCl the protection was also attempted with TBDMSOTf in the presence of lutidine (Scheme 19). This resulted in the protected compound **36** contaminated with silyl ether **38**. The formation of **38** was confirmed by mass spectrometry. Based on the ^{1}H NMR the yield of protected ether **36** was determined. Since purification by column chromatography on silica proved unable to separate the silyl ether from the product it was decided to attempt the bromination with the product mixture. Unfortunately treating the mixture with 1.0 eq. of bromine in chloroform for 22 h, no brominated product was detected.

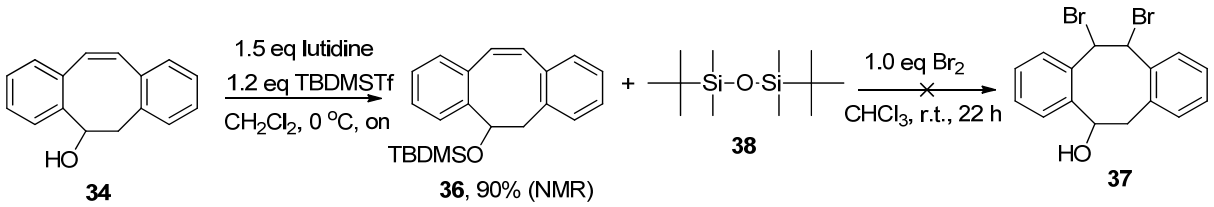

Scheme 19: Protection of alcohol 35 with TBDMSOTf and subsequent bromination.

The last step of the synthesis is the debromination resulting in final compound **11** (lit. 45%). Unfortunately only small amounts of **37** were synthesized, due to irreproducible reactions and long reaction times. The obtained **37** was only sufficient to obtain small crude samples of **11** according to ^{1}H NMR and mass. Unfortunately after column chromatography on silica no **11** was present.

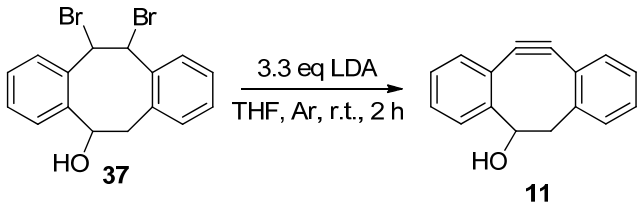

Scheme 20: Debromination of 11.

3.2 Synthesis of azocine

Due to the difficulties in the synthesis of **11**, another synthesis was attempted. During the struggles with the synthesis of **11**, the paper from Debets *et al.*[41] was published which contained a nine step synthesis to compound **39** in which all steps were reported with high yields.

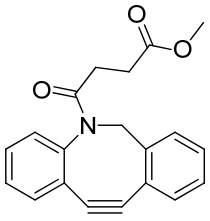

39

The first step described by Debets *et al.* is a Sonogashira coupling of iodide **45** and alkyne **44**, we were able to reproduce this coupling with 72% yield (Scheme 22). Because of the high commercial price of alkyne **44**, it was decided to synthesize this from amine **40** and trimethylsilylacetylene **41** following the procedure by Sakai *et al.* (Scheme 21).[72] This consists of a Sonogashira coupling followed by deprotection of the trimethylsilyl group with KOH.

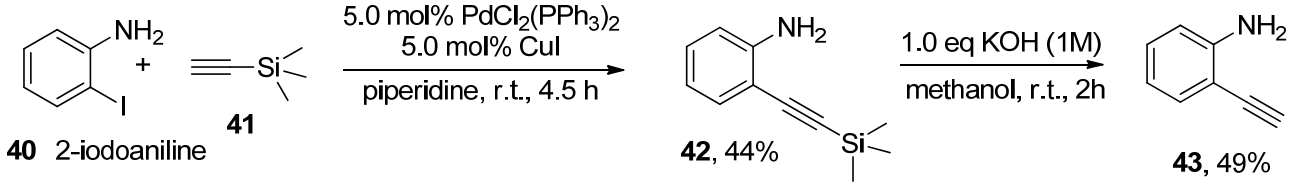

Scheme 21: Sonogashira coupling and subsequent deprotection.

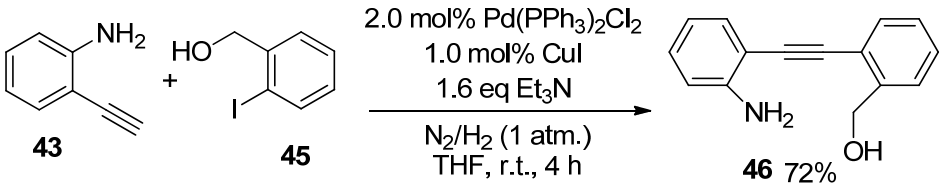

Scheme 22: Sonogashira coupling of alkyne 43 and iodide 45.

The reactions shown in Scheme 21 and 22 both entail a Sonogashira coupling.[73] This is a palladium catalyzed coupling of alkynes to aryl or vinyl halides. Often, as in our case, copper iodide is used as a co-catalyst. The mechanism of the copper co-catalyzed Sonogashira coupling reaction consists of two catalytic cycles (Scheme 23). Usually, on account of convenience, the more stable Pd(II), for instance $Pd(PPh_3)_2Cl_2$, is used instead of Pd(0). The Pd(II) species is then reduced *in situ* to the catalytically active Pd(0) species (**1**). The reactive Pd(0) species undergoes oxidative insertion of the organic halide yielding an intermediate Pd(II) species (**2**). In the copper catalyzed cycle the alkyne complexes with CuI(**1'**). This complex is deprotonated by a base (**2'**). The resulting Cu-alkyne species undergoes transmetallation with the Pd(II) species (**3**), resulting in regeneration of CuI and formation of the Pd(II)-alkyne species. The Pd(II)-alkyne species undergoes reductive elimination yielding the product and regenerating the active Pd(0) species (**4**). A major advantage of the Sonogashira coupling is that it can take place under mild reaction conditions, so it can be used for thermally sensitive substrates.[74]

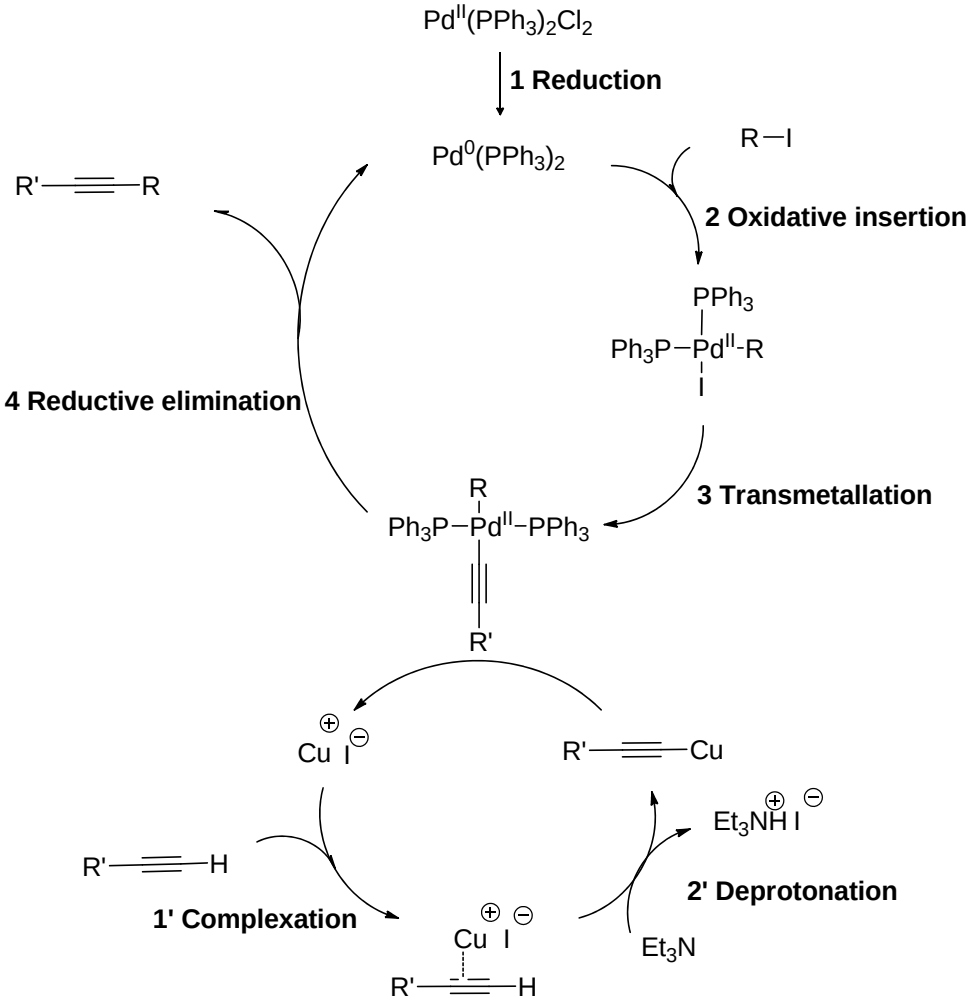

Scheme 23: Mechanism of the copper co-catalyzed Sonogashira reaction.

The Sonogashira coupling shown in scheme 22 is executed in a N_2/H_2 atmosphere while the Sonogashira coupling usually takes place in inert (N_2) atmosphere. Debets *et al.* use a N_2/H_2 atmosphere to prevent the Glaser coupling, a coupling of two alkynes yielding the homocoupled 1,3-diyne (Scheme 24). During the Sonogashira coupling the Cu-alkyne intermediate is also formed and Debets *et al.* found that without the reductive H_2 atmosphere the Cu-alkyne complexes are able to form the diyne which usually only happens under oxidative conditions. Unfortunately the mechanism of the Glaser coupling in not fully understood, so it is difficult to say how the H_2 atmosphere prevents the diyne formation.[75]

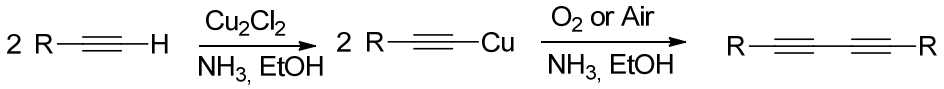

Scheme 24: Glaser coupling yielding the homocoupled 1,3-diyne.

After formation of acetylene **46** via the Sonogashira coupling the amine is protected with a Boc group. This is done by reacting the free amine with an equivalent of Boc anhydride in THF at 70°C for 2 days, giving the product in 97% yield (Scheme 25). The protection is necessary for the eventual oxidation of the alcohol, but prior to the oxidation the internal alkyne is hydrogenated to the alkene. The 15% improvement of yield with regard to the literature comes from using a different purification method. In stead of column chromatography the product is purified by washing with citric acid, this gives the same product according to ^{1}H NMR in higher yield.

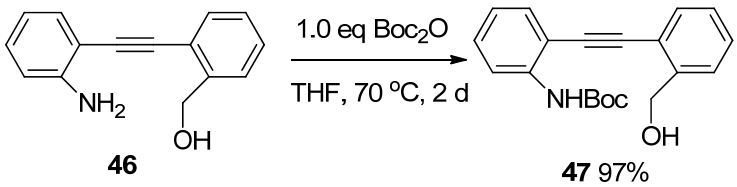

46 **47** 97%

Scheme 25: Protection of amine 46.

Hydrogenation of unsaturated bonds often takes place under a hydrogen atmosphere in the presence of a palladium catalyst. In this case only hydrogenation to the alkene is desired. Since the alkene can also be hydrogenated to the alkane under the same conditions a selective catalyst is needed. Fortunately alkynes are slightly more reactive towards hydrogenation than alkenes allowing for selective hydrogenation.[74]

The mechanism of this type of hydrogenation is shown in Scheme 26. The first step is the adsorption of hydrogen on the catalyst surface, then the alkene (or alkyne) coordinates to the surface. Subsequently the two hydrogens are transferred to the alkene yielding the *syn*-alkane. Since the reaction takes place on the surface, the reaction is best catalyzed if the catalyst is finely divided. This is why the catalyst is often mixed with a support, in this case the palladium particles are deposited on a support of powdered barium sulfate.[74]

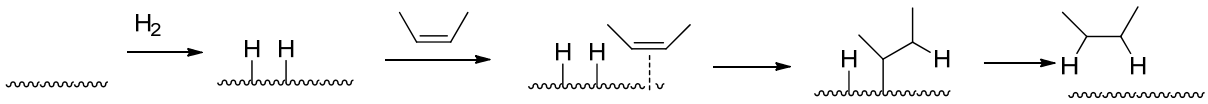

Scheme 26: Mechanism of the hydrogenation of a double bond.

To achieve selective hydrogenation, a less active catalyst is needed. A famous chemoselective catalyst is Lindlar's catalyst, a palladium catalyst poisoned with lead. Another possibility to posion

the catalyst is to add quinoline. These poisoned catalysts can still convert, although significantly more slowly, the alkene to the alkane so these reactions always requires careful monitoring.[74]

The chemoselective system used by Debets *et al.* to convert alkyne **47** to alkene **48** is 1 mol% of 10% Pd/$BaSO_4$ with quinoline in methanol, giving the product with 95% yield. Unfortunately when similar conditions were tried, 1 mol% of 5% Pd/$BaSO_4$ with quinoline in methanol, the ^1H NMR showed a conversion of only 9%. Other conditions were tested to optimize the reaction, as listed in Table 2.

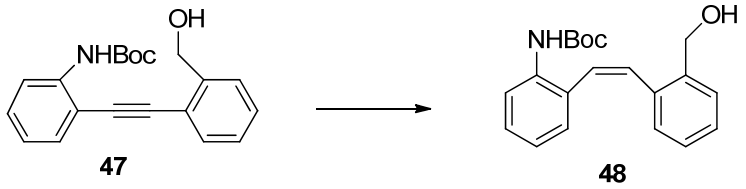

Entry	Conditions	Remarks
1	1 mol% Pd on $BaSO_4$(5%), 1% quinoline, 1.5 h, r.t, 1 atm. H_2	^1H NMR shows ~ 9% conv.
2	1 mol% Pd on $BaSO_4$(5%), 1% quinoline, 3 h, r.t, 1 atm. H_2	^1H NMR shows ~ 10 % conv.
3	10 mol% Pd on $BaSO_4$(5%) (in 3 x), No quinoline, 48 h, after 18 h heated to 40 °C, 1 atm. H_2	^1H NMR shows ~ 90% conversion to the alkane
4	1 mol% Pd on $BaSO_4$ (10%), large excess of quinoline, 4 h, r.t., 1 atm. H_2	^1H NMR shows only sm and quinoline
5	1 mol% Pd on $BaSO_4$ (10%), 1% quinoline, 8 h, r.t., 1 atm. H_2	^1H NMR shows 2:1 sm and product
6	2% $Ni(OAc)_2$, Ethylenediamine, $NaBH_4$, 23 h, r.t., 1 atm. H_2	TLC and crude ^1H NMR show no conversion
7	3.3 mol% Pd on $BaSO_4$ (10%), 33 mol% quinoline, 20 h, r.t., 1 atm. H_2	Only product visible on ^1H NMR

Scheme 27: hydrogenation of compound 47 to alkene 48.

Table 2: Conditions for the hydrogenation of compound 47, Scheme 27.

After the first attempt (entry 1) the reaction time was doubled to see if more product was formed. Since this did not yield more product it was hypothesized that the quinoline might be too effective in poisoning the catalyst. It was therefore attempted to force the reaction to completion with large amounts of palladium, in the absence of quinoline and longer reaction times. This resulted in 90% conversion to the alkane.

The next attempt was to use 10% Pd/$BaSO_4$, as described in the literature procedure, instead of 5% Pd/$BaSO_4$ but this did not result in more conversion either (entry 4). Increasing the reaction time

to 8 h resulted in a 2:1 mixture of starting material and product so this was clearly a step in the right direction. Another catalyst system comprising a Ni catalyst was also tried but this showed no conversion. Stirring the reaction mixture for 20 hours with a slightly higher mol% of palladium showed full conversion (entry 7) so these conditions were chosen for the reaction, this gave the isolated product in 52% yield (Scheme 28).

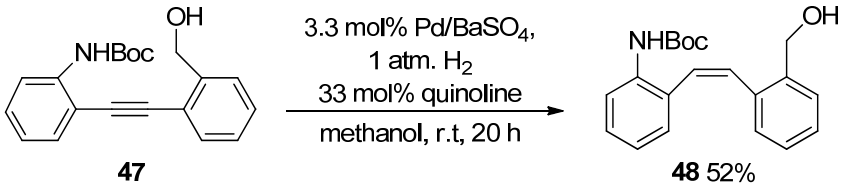

Scheme 28: Final conditions for the conversion of alkyne 47 to alkene 48.

After the hydrogenation to the double bond, the free alcohol was oxidized to the aldehyde with Dess-Martin periodinane (DMP). With 1.2 equivalents of the periodinane and excess base the alcohol was transformed in 3.5 h at room temperature to the corresponding aldehyde in 93% yield (Scheme 29).

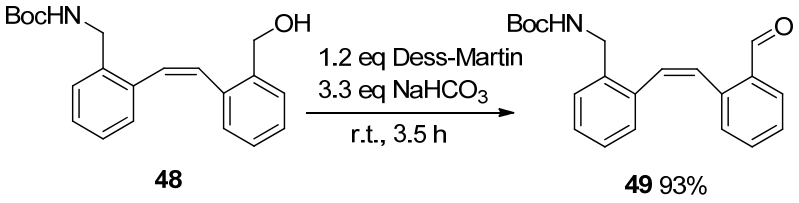

Scheme 29: Dess-Martin oxidation of 48.

DMP is a salt that is commercially available in a solution. The periodinane reacts in stochiometric amounts with the alcohol yielding the corresponding carbonyl compound and iodinane. ^{1}H NMR studies have shown that when twice as much alcohol is present with respect to the DMP, double displacement occurs resulting in the formation of acetoxydialkyloxiperiodinane. This supports the formation of the diacetoxyalkyloxiperiodinane intermediate, which is subsequently deprotonated by the acetate anion resulting in final products (Scheme 30).[75]

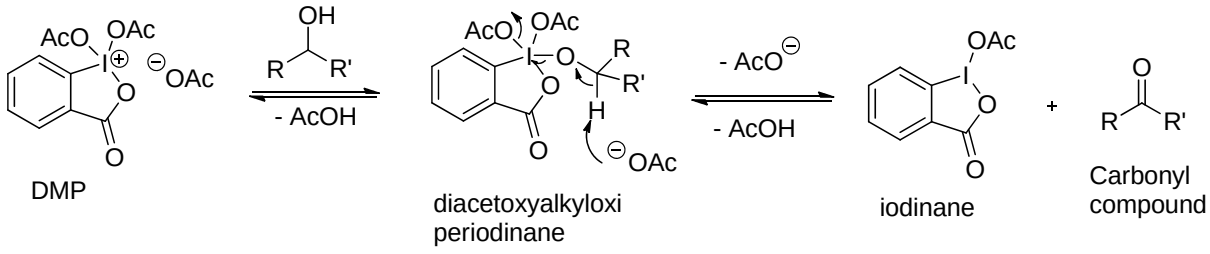

Scheme 30: Mechanism of the Dess-Martin oxidationof an alcohol to a carbonyl compound.

Once the aldehyde is in place, a one-pot deprotection, reductive amination reaction is performed. The Boc protecting group can easily be removed by treatment with hydrochloric acid. Subsequently the free amine can attack the aldehyde resulting in ring closing. The intermediate imine, reported by Debets *et al.*, is not isolated but directly treated with sodium borohydrate resulting in reduction of the imine to the free secondary amine. After washing the reaction mixture with water and brine the ^{1}H NMR showed pure **50** in quantitative yield.

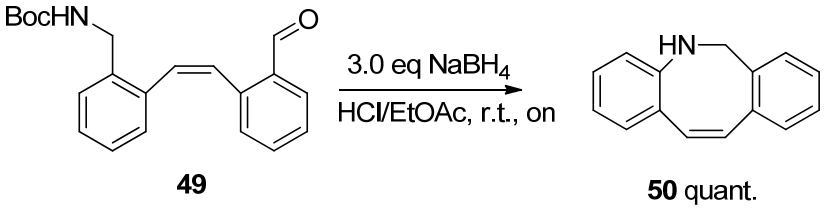

Scheme 31: Deprotection and reductive amination to obtain 50.

The mechanism of the deprotection and subsequent ringclosing starts with activation of the carbonyl *via* protonation by the acid. Then, upon loss of a tert-butyl carbocation, the carboxylic acid is formed. The tert-butyl carbocation forms isobutene upon regeneration of the catalytic proton. Deprotonation of the acid by the amine and subsequent loss of CO_2 results in formation of the free amine.

The amine can than attack the aldehyde resulting in the hemiaminal intermediate. The alcohol can be protonated by the acid making it a better leaving group. The amine donates its lone pair resulting in loss of water and formation of an imine. The imine is then attacked by the reducing agent borohydride, resulting in reduction of the imine to the secondary amine **50** (Scheme 32).[74]

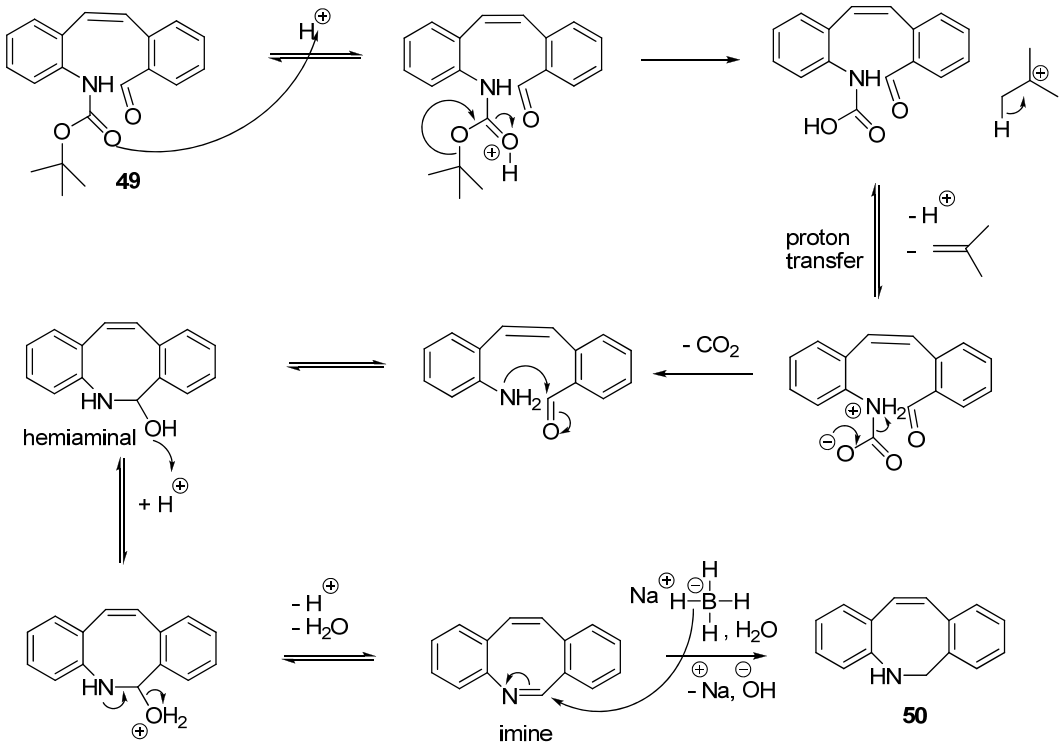

Scheme 32: Mechanism of the deprotection of 49 and subsequent reductive amination, resulting in 8-membered ring compound 50.

The literature reports that direct bromination of alkene **50**, resulted in an intramolecular attack of the amine resulting in the formation of an indoline.[41] Therefore the amine was first protected as an amide by letting it react with succinimyl chloride, giving the corresponding amide in 60% yield (Scheme 33). The mechanism is a nucleophilic attack of the amine on the carbonyl moiety with chloride acting as the leaving group. The group of Debets et al. used a different protecting group (with one carbon more), therefore compound 50 is a new compound and was fully characterized by ^{1}H NMR, ^{13}C NMR and mass.

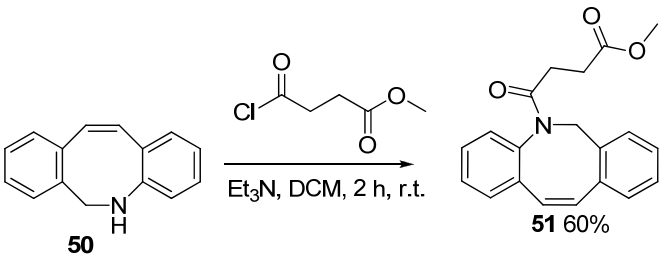

50 **51** 60%

Scheme 33: Protection of the secondary amine as an amide yielding compound 51.

After protection of the amine the double bond could be brominated in quantitative yield resulting in the dibromo compound **52** (Scheme 34). Bromination of the double bonds begins with attack of the double bond on the bromine, resulting in the formation of a bromonium ion and a bromide ion. The bromonium ion is subsequently attacked by the bromide ion resulting in the debrominated compound (Scheme 35).[74]

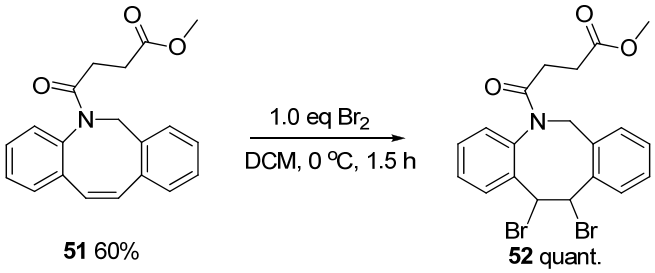

51 60% **52** quant.

Scheme 34: Bromination of 51.

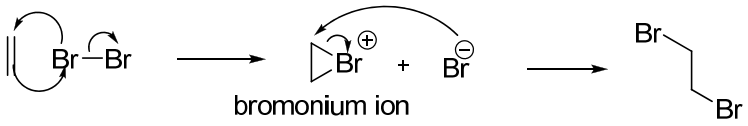

Scheme 35: Reaction mechanism of the addition of bromine to a double bond.

The last step in the synthesis of cyclooctyne **39** is the debromination of compound **52**. The formation of cyclooctyne **39** occurs *via* two subsequent elimination reactions (Scheme 36 and 37). The reaction occurs in the presence of a base, in this case potassium *tert*-butoxide, which attacks one of the protons on the bromide substituted carbon, resulting in the formation of a double bond and loss of a bromine ion. Since another bromine is still present a second elimination occurs resulting in formation of the alkyne. The obtained target molecule **39** was fully characterized by ^{1}H NMR, ^{13}C NMR and mass. Compound **39** proved to be stable at 5 °C for several months.

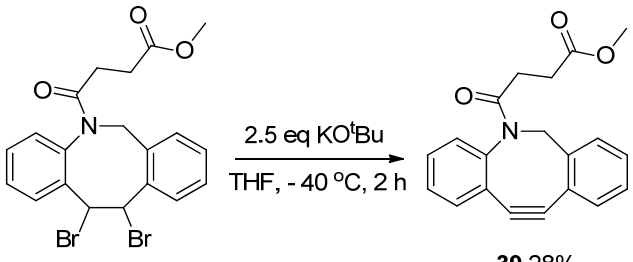

52 **39** 28%

Scheme 36: Debromination of 51.

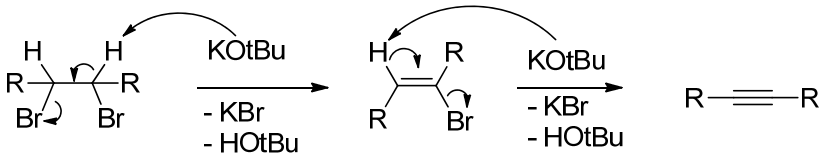

Scheme 37: Mechanism of debromination.

3.3 Clicking azocine

To see if the cyclooctyne is reactive enough to 'click' to an azide within the desired timescale the cyclooctyne is clicked to *para*-fluoro-azidobenzene **53** (Scheme 38). The reaction takes place in an NMR tube and is followed by ^{1}H NMR over a period of an hour. Subsequently the signals of the two benzylic protons of compound **39** and the benzylic protons of both regioisomers of the product **54** are integrated. Since the initial concentrations are known the integrals could be converted to concentrations, assuming that the sum of the concentrations of **39** and **54** remains constant. Graph 1 shows the change in concentration of the product and the cyclooctyne in time.

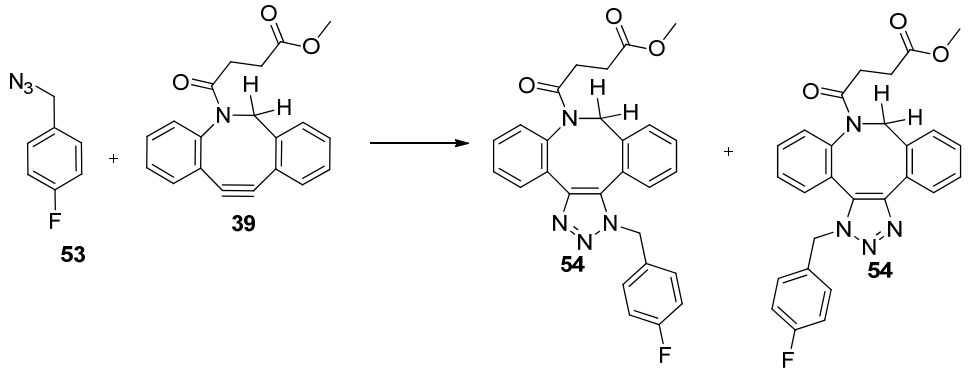

Scheme 38: 'Click' reaction between cyclooctyne 39 and fluorinated compound 53.

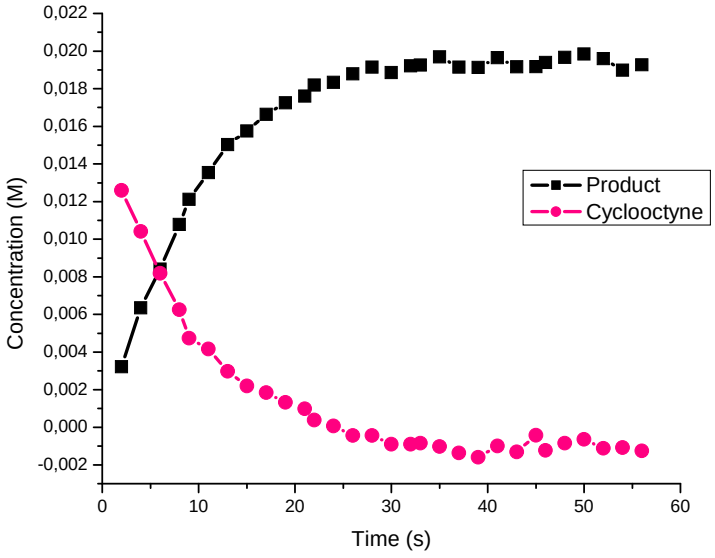

Graph 1: Reaction progress measured by ^{1}H NMR.

When the conversion is plotted against time Graph 2 is obtained. From this graph it can be seen that the reaction reaches full conversion after 30 min. and that 90% conversion is already reached after 20 min. This is a promising time scale for the work with the radioactive label ^{18}F.

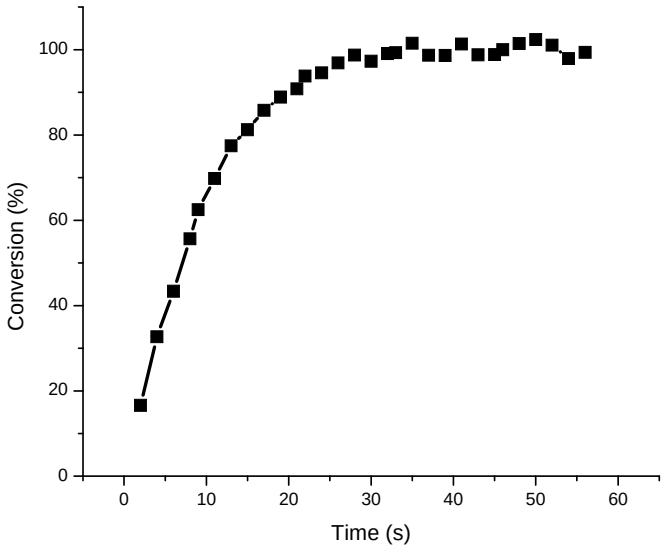

Graph 2: Conversion of the 'click' reaction between 39 and 53 as a function of time.

Because of the promising rate of the reaction, cyclooctyne **39** was clicked to [^{18}F] labeled molecules to determine the radiochemical yield. These radiolabeled 'click' reactions were preformed at the UMCG by Leila Mirfeizi. First two different radiolabeled azides were synthesized (Scheme 39). Once formed, the labels were clicked to cyclooctyne **39** in a DMSO/H_2O (1/3) mixture for 15 min. at room temperature resulting in compounds **59** – **60** with radiochemical yields between 31-44%. The radiochemical yields of 25 to 44% are not exceptionally high but they are promising and a good starting point for further attempts to use the Cu-free AAC for PET labeling.

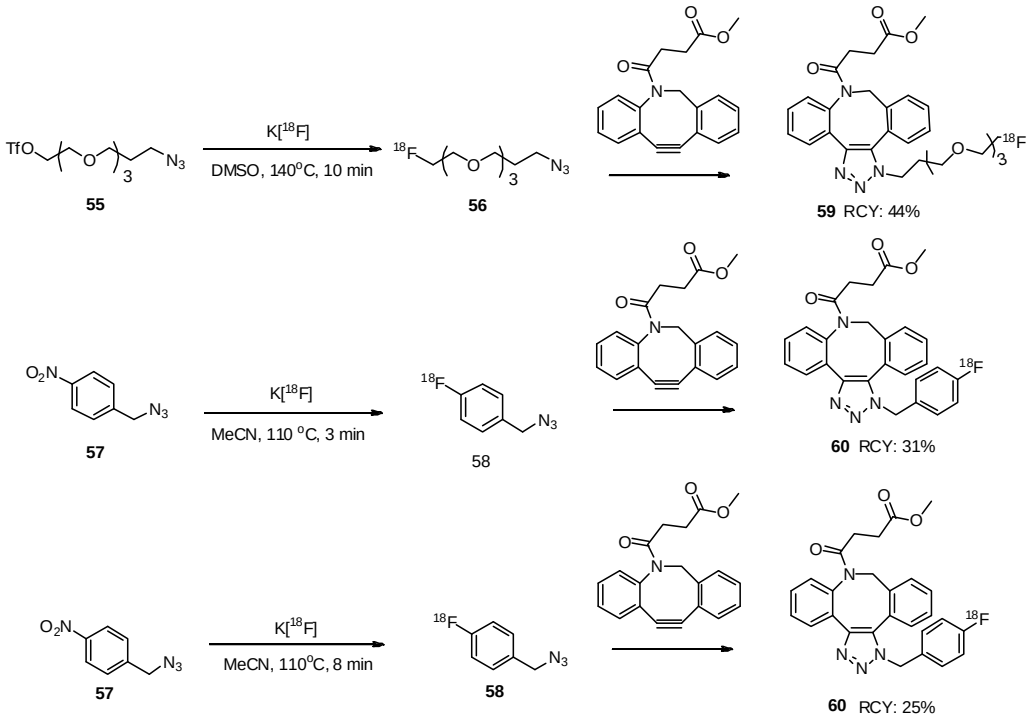

Scheme 39: Synthesis of ^{18}F labeled compounds to click to cyclooctyne 39.

In conclusion a new strained cyclooctyne **39** was successfully synthesized and proved to be stable for several months when it was stored at 5 °C. It's structure was confirmed by ^{1}H NMR, ^{13}C NMR and mass. Following the 'click' reaction of the strained cyclooctyne **39** with azide **53** by ^{1}H NMR showed that 90% conversion is reached in 20 min.. Subsequently compound **39** was given to the UMCG were it was 'clicked' to radiolabeled azides **55** and **57**. These test reactions gave good RCY thereby paving the way for *in vitro* and later *in vivo* studies.

4 Combining fluorescence with PET

As shown in the introduction, combining imaging techniques is very valuable for the detection and treatment of disease. So far, few efforts have been made for the development of multi-modality probes for combining PET and optical imaging. What has been done focuses on the longer lived metal isotopes like ^{64}Cu for reasons of synthetic convenience. The drawbacks of the use of these long lived isotopes is that the patient is subjected longer to the radioactivity and that metals like copper are cytotoxic, even when their radioactivity has decayed. Furthermore metallic ions are capable of changing metabolites significantly and they give cross complexation with other proteins.[65]

The goal of this part of the research is to develop a multi-modality probe that makes use of the short lived radioisotope ^{18}F. The synthetic difficulties that arise with the use of short lived radioisotopes are hopefully overcome by introducing the radioactive label as a last step *via* 'click'chemistry.

4.1 Functionalization of coumarins and perylenes

There are many fluorescent dyes available and since a 'click' handle is needed for future attachment to a radioactive label, the alkyne containing coumarins synthesized by Sivakumar *et al.*[76] provided a good starting point. Schiedel *et al.*[77] showed in 2001 the fluorescent abilities of a wide variety of coumarins. The coumarins have an emission maxima between 400-569 nm, so well within the visible region and showed generally good quantum yields ranging from 0.26 to 0.98. Sivakumar *et al.* introduced an azide moiety on several coumarins and 'clicked' them to a variety of small alkynes. They showed that the electron withdrawing azide quenches the fluorescence of the coumarin but that the triazole does not have this effect. This gives rise to a probe that only fluoresces once it is 'clicked'.

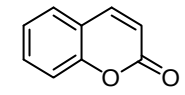

coumarin scafold

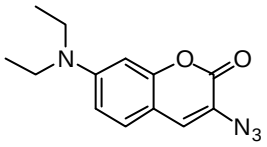

target molecule **61**

4.1.1 Synthesis of 3-azido-7-diethylaminocoumarin

Of all the 3-azidocoumarins synthesized by Sivakumar *et al.* 3-azido-7-diethylaminocoumarin **61** was selected because it showed strong fluorescence when 'clicked' to a variety of different substrates. Furthermore the synthesis of coumarin **61** is relatively straightforward. The synthesis of the azidocoumarin starts with the reaction of salicylaldehyde **62** with ethylnitroacetate **63** (Scheme 40).

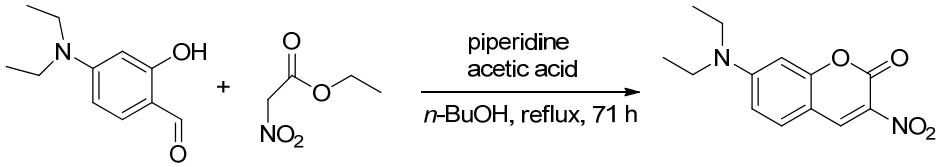

62 **63** **64**, 62%

Scheme 40: Reaction of salicylaldehyde 62 with ethylnitroacetate 63.

The mechanism of the formation of nitrocoumarin **64** starts with the protonation of the carbonyl of nitroacetate **63**. This activates the carbonyl towards nucleophilic attack by the hydroxyl group of the salicylaldehyde **62**. Upon loss of an ethanol molecule the carbonyl function is reformed and the molecule can undergo an intramolecular aldol reaction. First piperidine abstracts the α-proton resulting in the enolate. Subsequently the enolate attacks the carbonyl resulting in the formation of a lactone ring. Since another α-proton is present the piperidine can abstract another proton, forming again the enolate, then upon reformation of the ketone the hydroxyl group can act as an leaving group, producing α,β-unsaturated ketone **64** and a water molecule (Scheme 41).

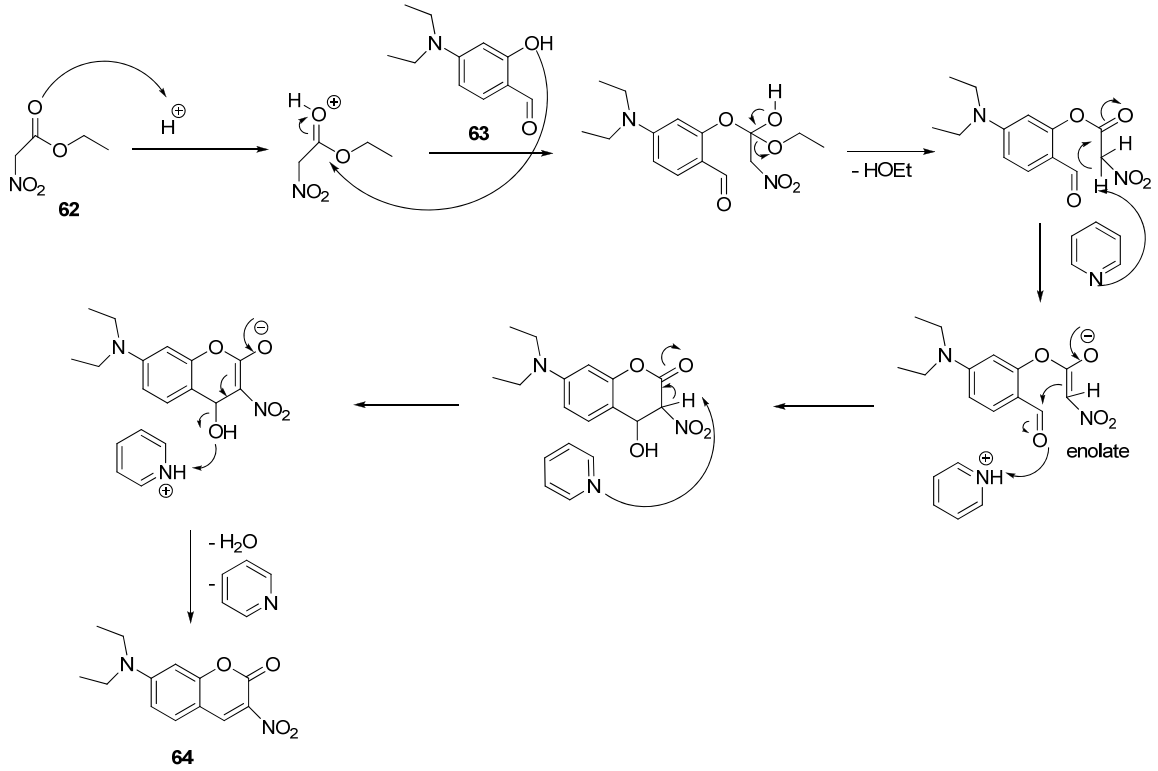

Scheme 41: Mechanism of the formation of nitro-coumarin 64.

Nitrocoumarin **64** was reduced to the corresponding amine **65** in 65% yield with $SnCl_2$ (Scheme 42). In this case the $SnCl_2$/HCl combination is used to selectively reduce the nitro group and leave the carbonyl group untouched. The mechanism involves the donation of electrons by the $SnCl_2$ and proton donation by the acid resulting in the loss of two equivalents of water and the formation of the amine compound.

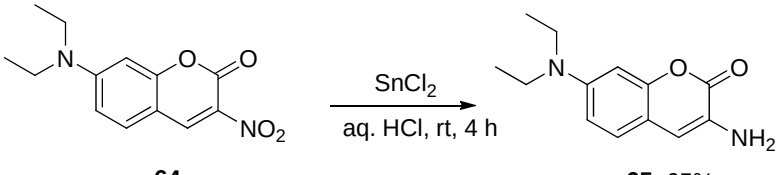

64 **65**, 65%

Scheme 42: Conversion of nitrocoumarin 64 to aminocoumarin 65.

The final step is the conversion of the amine to the azide (Scheme 43). The conversion of the amine to the azides occurs in three steps. The first step is the formation of ^{+}NO by adding $NaNO_2$ to a acidic solution. Subsequently the ^{+}NO is attacked by the amine of compound **65**. *Via* proton

loss, proton transfer, protonation of the oxygen and finally loss of a water molecule a diazonium salt is formed.

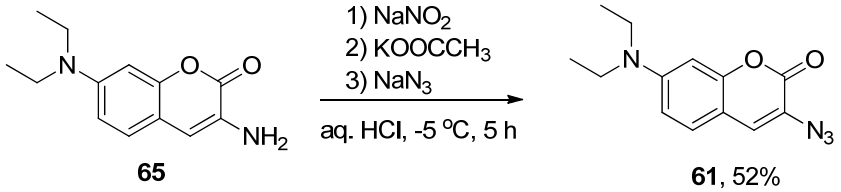

Scheme 43: Conversion of amine-coumarin 65 to azido-coumarin 61.

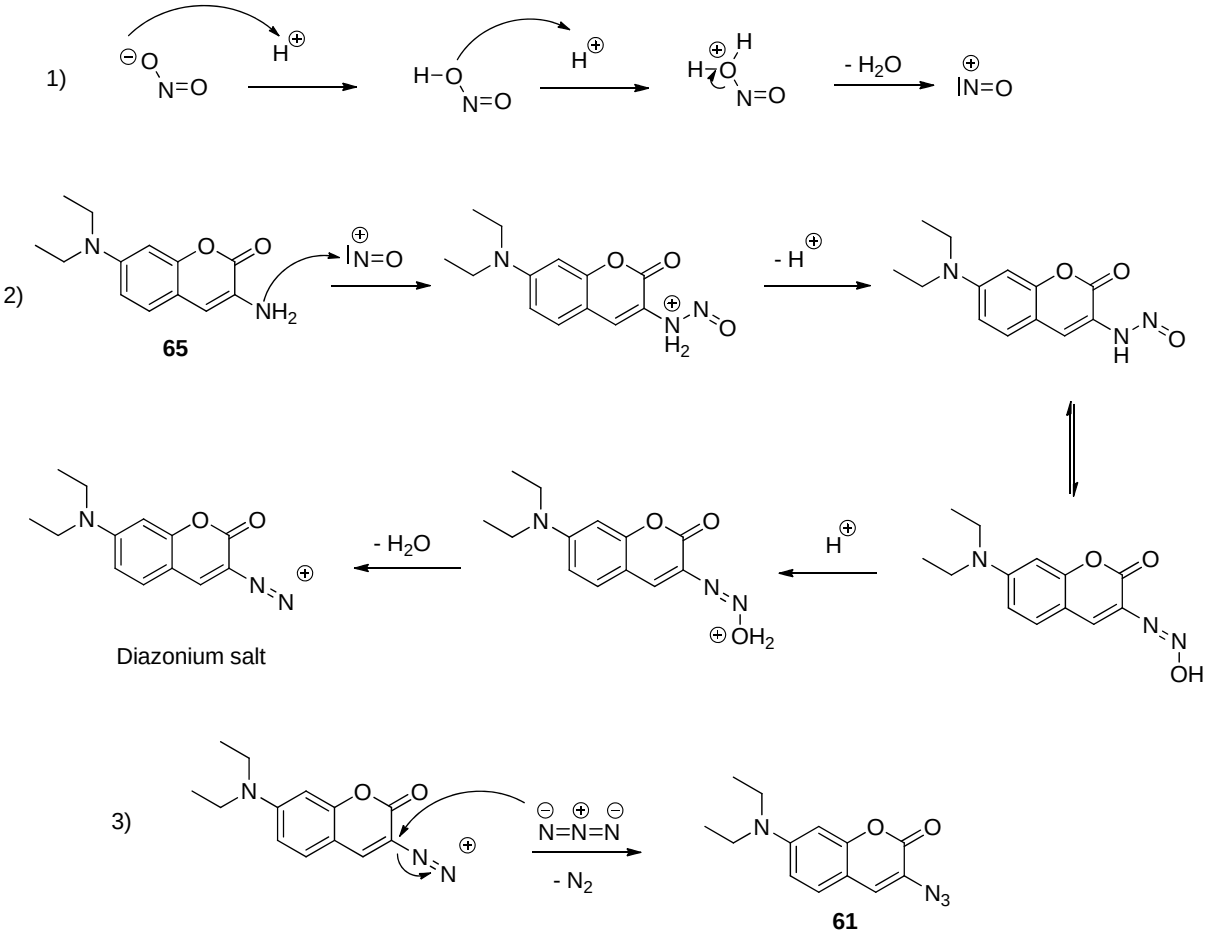

Scheme 44: Mechanism of the diazotization of the aromatic amine and the subsequent nucleophilic substitution by sodium azide and loss of N_2.

The diazonium salt readily undergoes nucleophilic attack since the leaving group is nitrogen gas. So when the diazonium salt is treated with sodium azide, which supplies an azide ion (which is a linear triatomic species that is nucleophilic at both ends),[74] the desired azide product **61** is formed.

Subsequently it was attempted to click the azido-coumarin **61** to phenylacetylene. Sivakumar *et al.* 'click' these compounds in the presence of 5 mol% copper catalyst. This reaction takes 12 h to go to completion (84% yield).[76] For the use of radioactive ^{18}F a shorter reaction time is needed. To accelerate the reaction the MonoPhos system by Feringa *et al.* was investigated.[14]

MonoPhos **66** can be synthesized in one step by stirring racemic binap **67** with hexamethylphosphortriamine **68**, in refluxing toluene solution for 61 h (Scheme 45). The product

was obtained in 45% yield and could be used as a ligand in the 'click' reaction of fluorophore **61** and phenylacetylene (Scheme 46).

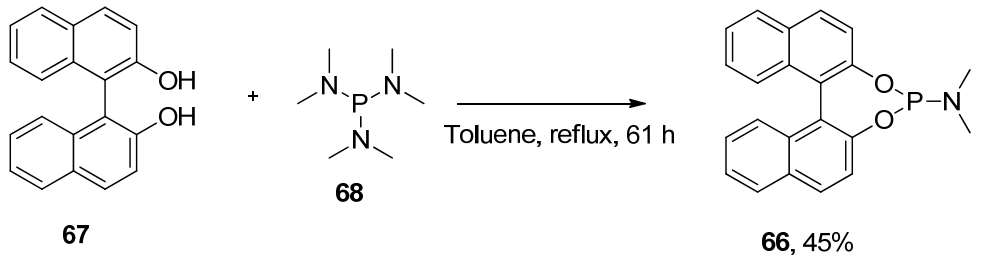

Scheme 45: Synthesis of MonoPhos 66.

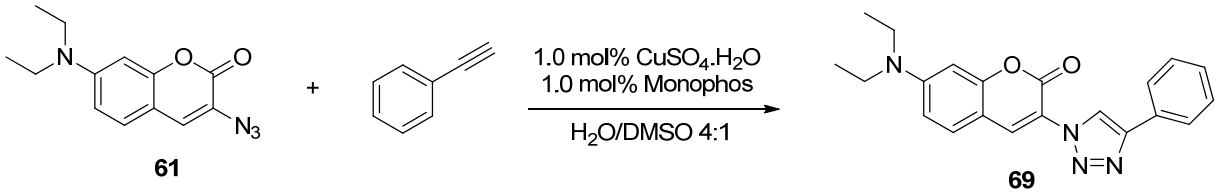

Scheme 46: Attempted synthesis of triazole 69.

Small aliquots were taken during the reaction to determine the conversion. Unfortunately the formation of product did not proceed faster in the presence of the MonoPhos ligand. Since a large rate acceleration of the 'click' reaction is necessary for the application in PET labeling a different system was sought.

4.1.2 Perylenes

Perylenes are polyaromatic hydrocarbons (PAH's) that fluoresce strongly and are therefore interesting for imaging. Since a perylene molecule itself does not contain functional groups that facilitate the connection to a molecule of interest often perylene diimides are used. Perylene diimides are well-known fluorescent dyes that contain high quantum yields and contain a remarkable chemical- and photostability.[78, 79]

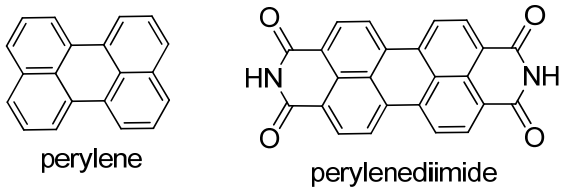

The synthesis of perylenediimides can be difficult and low yielding. Therefore we are grateful to Artem Kulago from whom we obtained perylenediimide **70**. To obtain the azido perylenediimide **71** a nucleophilic substitution with sodium azide was attempted (Scheme 47).

First the starting material was stirred with the nucleophile in acetone for 22 h at room temperature. When the resulting mixture was analyzed with ^{1}H NMR and IR only the starting material was found. Since no conversion was detected harsher methods were used. Entry 2 (Table 3) shows an attempt in a two layer system with the phase transfer catalyst Et_4NI to transfer the water soluble azide to the organic phase. After work up of the reaction, no azide was detected by

^{1}H NMR or IR. The reaction was also carried out in the polar solvent DMF at 80°C for 22 h. This attempt also showed no conversion by ^{1}H NMR or IR.

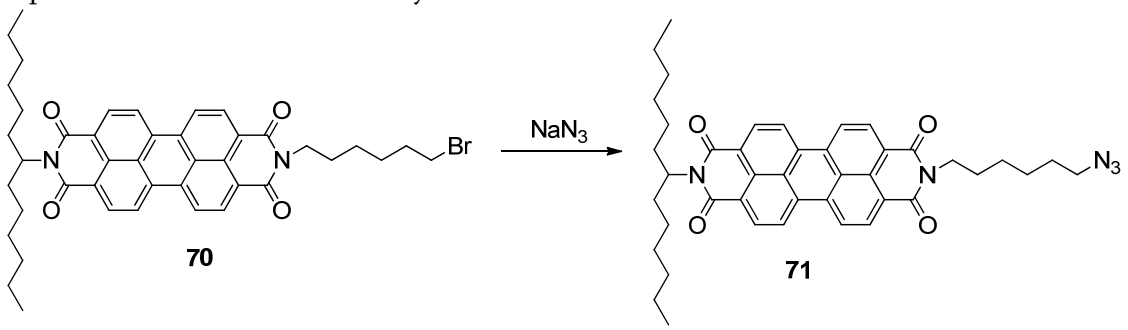

Scheme 47: Attempted conversion to azido perylene 71.

Entry	Eq. NaN_3	Solvent	Additives	Reaction time	Temperature
1	1.5	Acetone	None	22h	Rt
2	5	THF/H_2O	Et_4NI	67h	Reflux
3	1.1	DMF	None	22h	80°C

Table 3: Conditions for the attempted nucleophilic substitution by sodium azide.

When direct substitution proved to be unsuccessful a different leaving group, tosyl, was chosen. To introduce the tosyl group first the bromo functionality needed to be converted to the alcohol resulting in alcohol **72**. Due to the various functionalities in the molecule, mild conditions are desired for the conversion. Treatment with silver acetate and subsequent acidic work up yielded the desired product in 37% yield (Scheme 48).

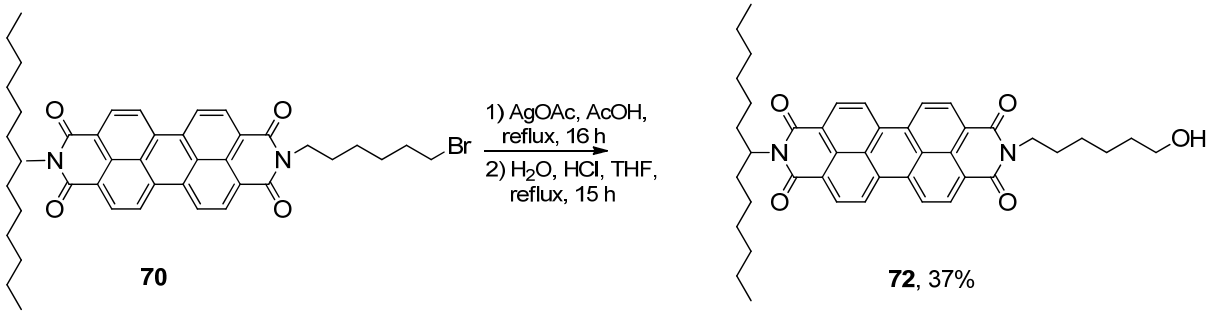

Scheme 48: Conversion of bromide 70 to alcohol 72.

This conversion starts with a nucleophilic attack of the acetate ion on the brominated carbon, resulting in loss of the bromide. This reaction is driven by the formation of the silver bromide salt which is insoluble and thus crashes out of solution. Once the acetate is formed it cannot go back to the bromide, pushing the reaction towards the product. After filtration to remove the salt the acetate is treated with acid in water. The acid activates the carbonyl compound making it a better leaving group, so water can attack carbonyl function resulting in the hydrolysis of the ester giving the alcohol and acetic acid (Scheme 49).

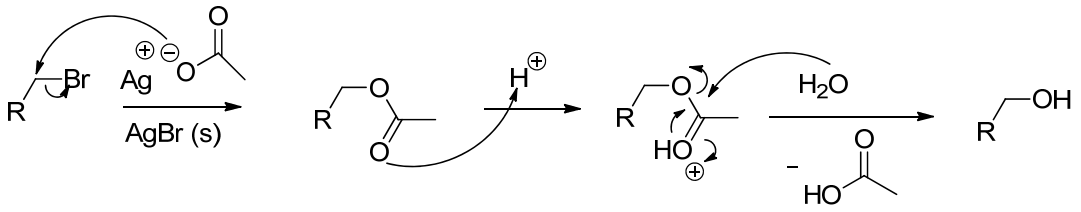

Scheme 49: Conversion of a bromo substituent to an alcohol.

Once the alcohol is formed it can be converted to the tosyl group by treating it with *para*-toluenesulfonyl chloride in dichloromethane (Scheme 50). Unfortunately due to the small scale, very little product was obtained so it was not possible to obtain an accurate yield. The mechanism proceeds *via* activation of the alcohol by abstraction of the proton by pyridine. The nucleophilic oxygen will subsequently attack the sulfur and upon loss of the chloro leaving group the desired product is formed (Scheme 51). Unfortunately the amount of product **73** was insufficient to allow for the next step, nucleophilic attack by the azide ion the form the desired azido compound **71**.

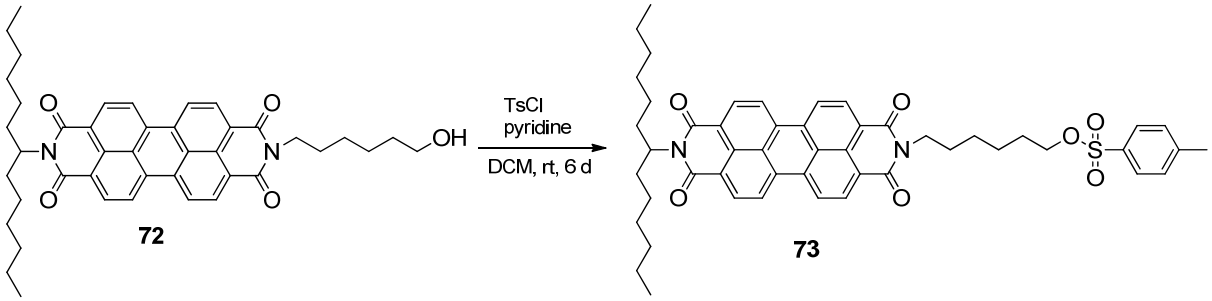

Scheme 50: Conversion of alcohol 72 to sulfonate 73.

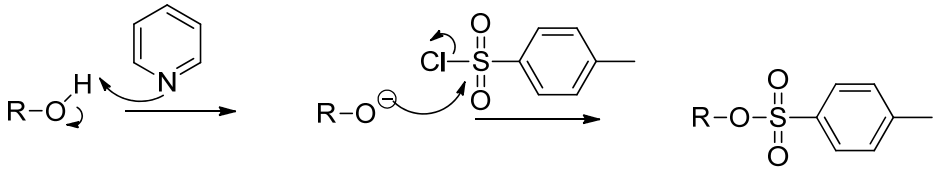

Scheme 51: Transformation of an alcohol to a tosylated group.

At this point a new strategy was devised. The main problem with the attempts so far was that even if it proved possible to 'click' a fluorinated compound to the fluorophore on an appropriate time scale nothing was gained as there would be no functional group left to connect a molecule of interest to the fluorophore-^{18}F construct.

4.3 The scaffold method

For a versatile dual modality probe 3 things are required: a fluorophore that has a high quantum yield and that is compatible with living systems, a functional group to which to attach the molecule of interest and a methodology to quickly attach the radioactive ^{18}F to the construct.

To achieve this it was decided to start with 3,5-diaminobenzoic acid **73**, and attach a fluorophore, a molecule of interest and a 'click' handle to the three functional groups present. Fluorophore fluorescein **74** was chosen. Fluorescein has an absorption (excitation) maximum around 494 nm which means it is easily excited by an argon-ion laser (488 nm). Furthermore it has an excellent quantum yield and is soluble in water, which is a necessity for the use in biological environments.[80, 81]

This isothiocyanate derivative of fluorescein is commercially available. It reacts readily with an amine group to form a thiourea linkage (Scheme 52). Fortunately the reaction mainly gave the mono substituted product. The mechanism starts with nucleophilic attack of the amine on the carbon of the isothiocyanate, resulting in formation of the thiourea compound (Scheme 53).

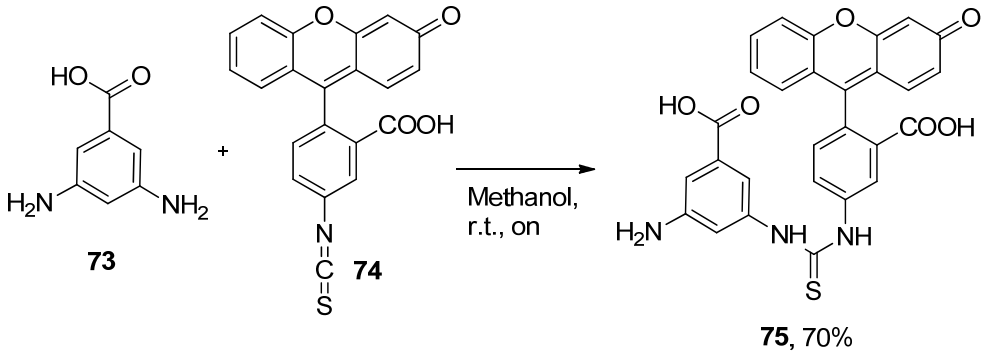

Scheme 52: Attaching the fluorescein to the scaffold.

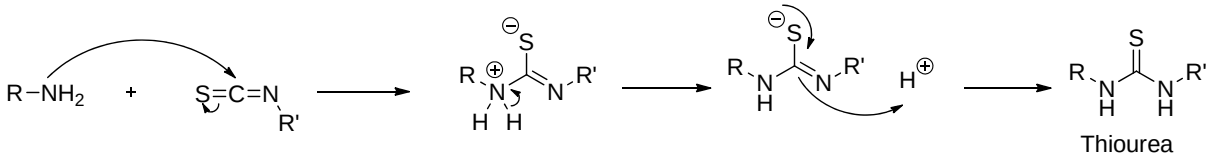

Scheme 53: Formation of thiourea bond from an amine and an isothiocyanate.

As a 'click' handle 4-pentynoic acid was chosen. To attach the acid via an amide bond to the free amine of scaffold **73**, the acid is first activated as its succinimyl ester following the procedure by Liu *et al*..[82] For the activation, acid **76** is stirred with an excess of *N*-hydroxysuccinimide **77** in the presence of 1-ethyl-3-(3-dimethylaminopropyl)carbodiimide (EDCI). Stirring at room temperature overnight resulted in 70% yield of the activated ester.

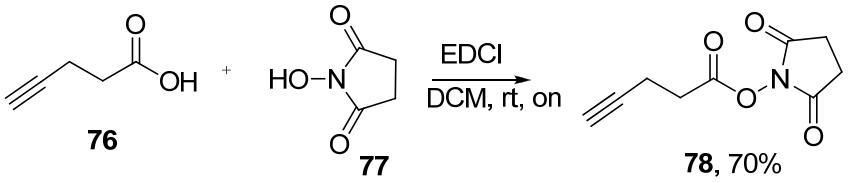

Scheme 54: Activation of 4-pentynoic acid.

The mechanism of the activation starts with the deprotonated acid that attacks the carbon of the carbodiimide, thereby activating the acid for nucleophilic attack. Upon nucleophilic attack by the hydroxyl functionality of *N*-hydroxysuccinimide on the carboxyl group, the "EDCI ester" acts as the leaving group resulting in the formation of the activated ester and the urea derivative of the carbodiimide (Scheme 55).[75]

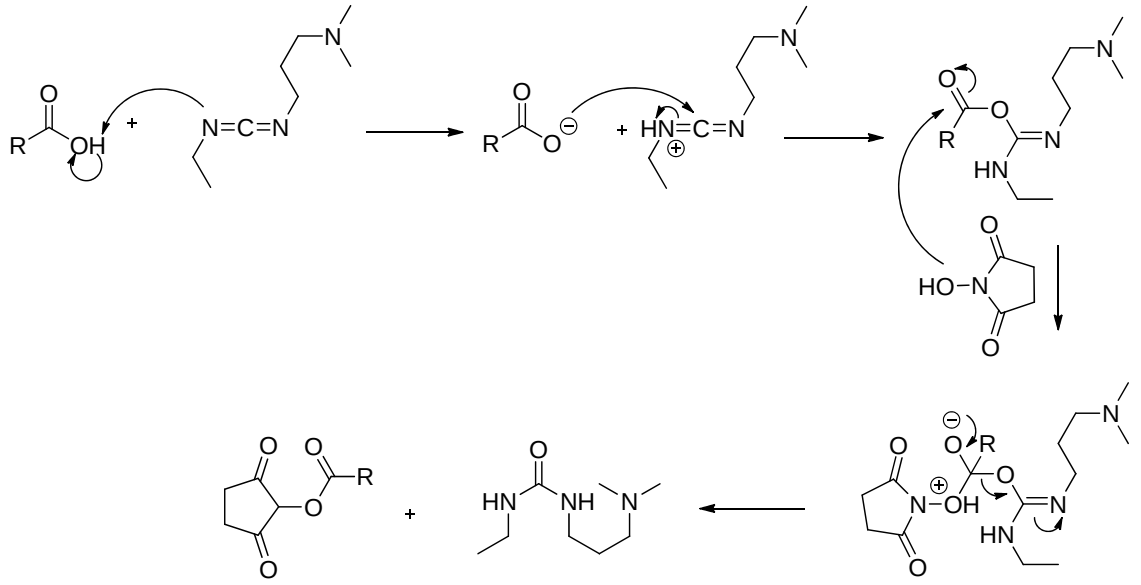

Scheme 55: Mechanism of the activation of an acid by EDCI and *N*-hydroxysuccinimide.

Once the activated ester was formed the formation of an ester bond between the scaffold **73** and the activated ester **78**. The activated ester was stirred with the scaffold and diisopropylethylamine (DIPEA) for three days at room temperature. Unfortunately no coupled product was detected under these conditions (Scheme 56). Regrettably lack of time resulted in no other conditions to synthesize compound **79**.

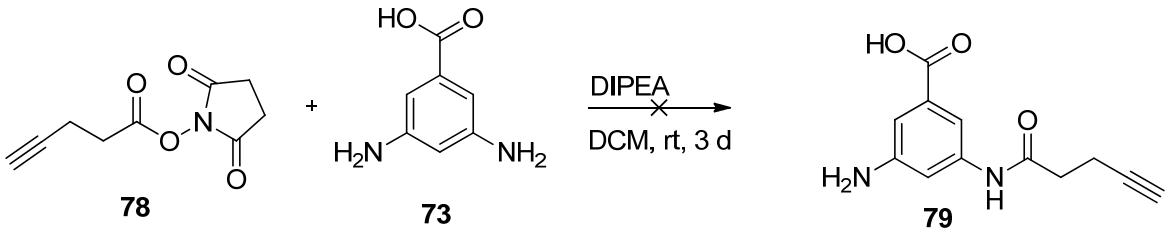

78 **73** **79**

Scheme 56: Attempted synthesis of 79.

5 Conclusions and outlook

The goal of this project was to synthesize a strained cyclooctyne that could be used for PET labeling. During this project strained cyclooctyne **39** was successfully synthesized. Furthermore experiments were done to determine the progress of the reaction in time. These experiments showed that the reaction of compound **39** with *p*-fluorobenzylazide occurs within 30 minutes, making it fast enough to use for test reactions with ^{18}F. These reactions with ^{18}F gave radio chemical yields between 25 and 44%. This is the first example of Cu-free AAC employed for ^{18}F PET labeling.

In the future the methyl esther of **39** can be hydrolyzed resulting in the free acid, to which a molecule of interest could be coupled. This could then be easily labeled by a Cu-free AAC with a ^{18}F azide (Scheme 57).

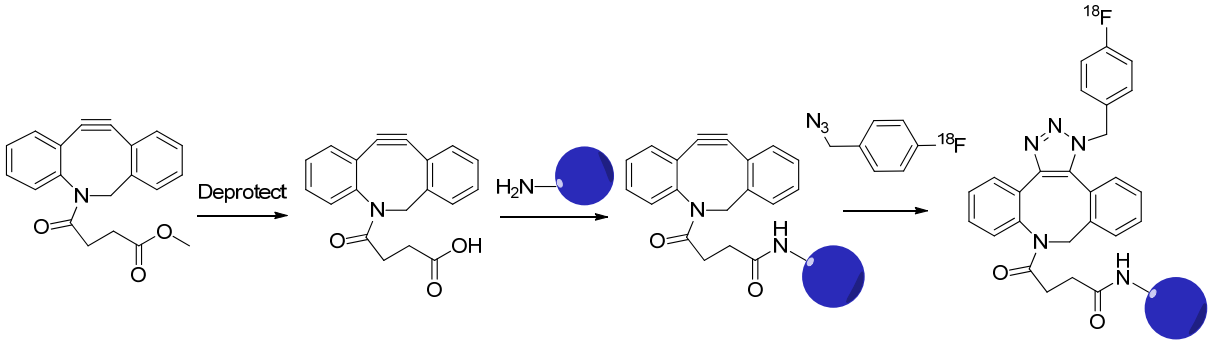

Scheme 57: Labeling target molecule with ^{18}F *via* the Cu-free AAC.

The second part of the project was to combine fluorescent labeling with PET by synthesizing a dual modality probe. Unfortunately due to limited time only initial reactions have been done for this project. But the 'scaffold' strategy, to start from a trifunctional aromatic system and attach all the desired functionalities is very versatile and promising. So far this research has shown that it is possible to synthesize the monosubstituted fluorescein-scaffold complex.

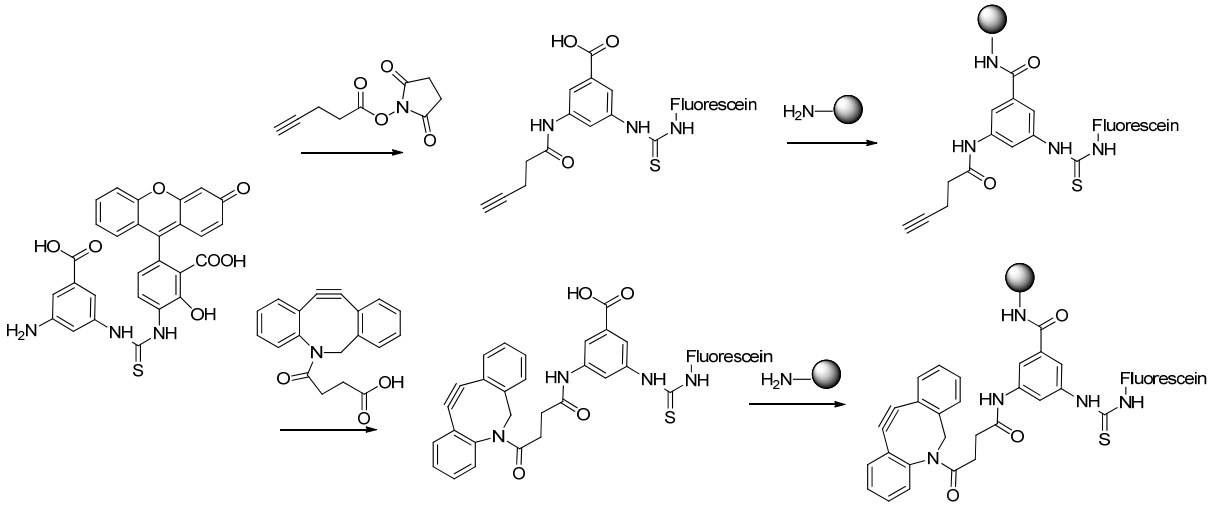

Scheme 58: Possible dual modality probes that can be labeled for PET *via* CuAAC and Cu-free AAC .

In theory it should be possible to also attach the activated ester **78** to the scaffold. In principle instead of this external alkyne, cyclooctyne **39** could be attached to the scaffold resulting in a Cu-free dual modality system. This system could be used for the visualization of many compounds and for this goal further research is being pursued.

6 Acknowledgements

As always research is a team effort and I would not have been able to do this research without the help of many others. First I would like to thank Lachlan for the daily guidance, without your constant help, suggestions and encouragement I would not have accomplished half of what is in this thesis. Hopefully now you have time for your own research again. I would also like to thank Ben Feringa for allowing me to do this project in his group and for his endless inspiration and love for chemistry.

Furthermore I would like to thank my labmates (Anne, Artem, Bea, Jack, Lachlan, Tati, Tim) for the great working atmosphere and Tim especially for always having everything that I needed in the lab. Also I would like to thank the Asymmetric Catalysis subgroup (Alena, Anne, Bin, Johannes, Lachlan, Maria, Martin, Pieter, Stella, Tim, Yi Ning, Yuange) and especially Adri Minnaard, for all the useful suggestions and discussions.

For all the help with the various apparatuses present in the lab I would like to thank Theodora (HPLC, GC, Mass), Tony (IR), Wesley (UV-VIS, fluorescence) and especially Pieter, Rene and Ruud for all their help and enormous patience when I tried to do NMR experiments.

My gratitude also goes to everybody present at coffee break, lunch break, football, workweek and all the other social activities at the Stratingh Institute you truly make being here a wonderful experience.

Last but definitely not least I would like to thank Dirk for putting up with me all the evenings that I got home drained and cranky from writing this thesis.

7 Experimental section

Chapter 3

3.1

2,3:6,7-Dibenzo-9-oxabicyclo[3.3.1]nona-2,6-diene 26 [39]

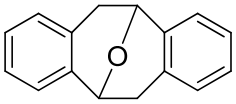

Phenylacetaldehyde **19** (4.8 g, 40 mmol) was dissolved in 20 ml dry DCM, under N_2 at 0°C. Subsequently the trimethylsilyliodide (6.5 ml, 48 mmol) was added and the mixture is stored at 5°C for 8 days. The reaction is quenched by addition of 40 ml of a 1M aq. solution of $Na_2S_2O_3$, and it is diluted with 40 ml DCM and stirred until the iodine color disappears. The layers are separated and the organic layer is dried with $MgSO_4$ and the solvent is removed. The crude product is purified by column chromatography on silica ($CHCl_3$) yielding 1.48 g of the product as a white solid (33%). R_f = 0.85 ^{1}H NMR (400 MHz, $CDCl_3$)δ 7.04-7.18 (m, 6H), 6.99 (d, J = 6.8 Hz, 2H), 5.32 (s, 2H), 3.57 (dd, J = 16.2, 6.8 Hz, 2H), 2.78 (d, J = 16.2 Hz, 2H).

3-Hydroxy-1,2:5,6-dibenzocycloocta-1,5,7-triene 34 [39]

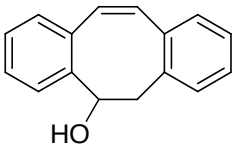

Compound **26** (300 mg, 1.19 mmol) was dissolved in 25 ml of dry THF under N_2 and the mixture was cooled to 0°C. Subsequently a 1.6M solution of n-BuLi in hexane (1.49 ml, 2.38 mmol) was slowly added to the mixture. The mixture was stirred for 4 h and then quenched with H_2O. The product was extracted from the mixture with 2 times 20 ml $CHCl_3$. The organic layers were washed with brine and dried with Na_2SO_4 and the solvent was removed under vacuo. The pure product was obtained by column chromatography on silica ($CHCl_3$) as a light yellow solid (196 mg, 74%). R_f = 0.38. ^{1}H NMR (400 MHz, $CDCl_3$)δ7.44 (m, 1H), 7.26-6.95 (m, 7H), 6.84 (d, J = 2.6 Hz, 2H), 5.26 (m, 1H), 3.38 (m, 2H), 1.84 (d, J = 5.2 Hz, 1H).

3-*tert*-Butyl-dimethylsilyl-oxy-1,2:5,6-dibenzocycloocta-1,5,7-triene 36 [39]

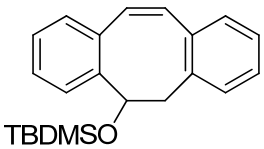

Method 1:
Compound **34** (196 mg, 0.88 mmol) was dissolved in 10 ml DCM and 2.5 ml pyridine, then *tert*-butylsylilchloride (266 mg, 1.77 mmol) was added. The reaction mixture was stirred for 22 h at room temperature. Subsequently the mixture was diluted with H_2O and the product was extracted with DCM (2 x 20 ml). The organic layers were washed with brine and dried over Na_2SO_4 and the

solvent was removed under reduced pressure. The product was purified by column chromatography on silica (heptane/EtOAc 7:1) yielding the product as a yellow oil 136.8 mg (46%). R_f = 0.13 ^{1}H NMR (400 MHz, $CDCl_3$)δ 7.73 (d, J = 7.7 Hz, 1H), 7.40 (t, J = 7.3 Hz, 1H), 7.32 (t, J = 7.3 Hz, 1H), 7.28-7.21 (m, 5H), 7.07 (d, J = 12.5 Hz, 1H), 6.98 (d, J = 12.5 Hz, 1H), 5.64 (dd, J = 9.5, 6.2 Hz, 1H), 3.67 (dd, J = 15.4, 6.2 Hz, 1H), 3.35 (dd, J = 15.4, 9.9 Hz, 1H), 1.10 (s, 15H).

Method 2:
Compound **34** (303 mg, 1.36 mmol) was dissolved in 8 ml dry DCM at 0°C 2,6-lutidine (2.37 ml, 2.05 mmol) and TBDMSOTf (433mg, 1.64 mmol) were added. The reaction misture was allowed to warm to room temperature and stirred for 17 h. Then the reaction was diluted with H_2O and extracted with DCM, washed with brine and dried with $MgSO_4$ and the solvent was evaporated. The crude product was purified by column chromatography on silica (pentane/EtOAc 7:1) yielding a mixture of the product R_f = 0.13 and silylether **38** R_f = 0.13 (632 mg).

3-Hydroxy-7,8-dibromo-1,2:5,6-dibenzocyclooctene 37 [39]

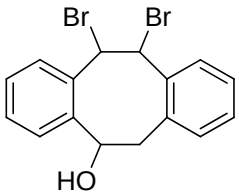

Method 1:
Compound **36** (137 mg, 0.41 mmol) was dissolved in 15 ml $CHCl_3$ and the solution was cooled to 0 °C. Then a solution of bromine (0.2 ml, 81 mmol) in $CHCl_3$ (1 ml) was added dropswise to the mixture. After stirring for 30 min the icebath was removed and the reaction mixture was stirred for an additional 22 h at room temperature. The reaction was quenched with 10 ml sat. aq. $Na_2S_2O_3$, then the layers were separated and the organic layer was dried and the solvent removed. The product was purified by column chromatography on silica (pentane/DCM, 7:1) yielding 149 mg, (45%). R_f = 0.58, ^{1}H NMR (400 MHz, $CDCl_3$) δ7.79 (d, J = 7.7 Hz, 1H), 7.20 (m, 1H), 7.11 (m, 1H), 7.03 (m, 3H), 6.91 (d, J = 7.3 Hz, 1H), 6.85 (d, J = 7.7 Hz, 1H), 6.45 (d, J = 9.9 Hz, 1H), 5.33 (d, J = 10.2 Hz, 1H), 5.28 (dd, J = 10.4, 9.3 Hz, 1H), 4.08 (dd, J = 14.8, 10.8 Hz, 1H), 3.72 (dd, J = 14.6, 9.1 Hz, 1H).

Method 2:
The mixture obtained by method 2 for the preparation of compound **36** (137 mg, 0.41 mmol) and silylether **38** was dissolved in 15 ml $CHCl_3$ and cooled to 0°C. Then a solution of bromine (0.2 ml, 81 mmol) in $CHCl_3$ (1 ml) was added dropswise to the mixture. After stirring for 30 min the icebath was removed and the reaction was stirred for an additional 22 h at room temperature. The reaction was quenched with 10 ml sat. aq. $Na_2S_2O_3$, then the layers were separated, the organic layer was dried and the solvent removed in vacuo. ^{1}H NMR, showed no product and no starting material.

3-Hydroxy-7,8-didehydro-1,2:5,6-dibenzocyclooctene 11 [39]

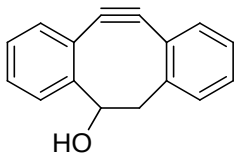

Compound **37** (140 mg, 0.37 mmol) was dissolved in 25 ml dry THF under N_2 with mol sieves present. A 2 M solution of LDA in THF (0.66 ml, 1.32 mmol) was added dropswise to the reaction which stirred for 2 h. Subsequently the mixture was poured over 20 ml ice water and extracted with DCM (2 x 50 ml). The organic layers were dried with $MgSO_4$ and the solvent was removed. The crude product was purified by column chromatography on silica (pentane/EtOAc, 5:1). Crude ^{1}H NMR showed product, but none was present after the column according to NMR and GC MS.

3.2

2-((triMethylsilyl)ethynyl)aniline 42 [72]

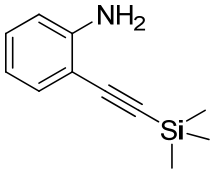

CuI (53 mg, 0.28 mmol) was suspended in 3 ml piperidine. Ethynyltrimethylsilane **41** (0.76 ml, 5.5 mmol) was dissolved in 3 ml piperidine and added to the CuI suspension. 2-Iodoaniline **40** (1.00 g, 4.6 mmol) was together with $PdCl_2(PPh_3)_2$ (196 mg, 0.28 mmol) was dissolved in 6 ml piperidine. After stirring both solutions for 3 h the aniline mixture was added to the acetylene mixture. The reaction mixture was stirred for 22 h, at which point the TLC showed full conversion of the starting material. Subsequently the reaction was quenched with saturated aqueous $NaHCO_3$. After extraction with DCM, three times, and drying over Na_2SO_4 the solvent was removed under reduced pressure. Column chromatography on silica (pentane/EtOAc 9:1) yielded the product as of white solid (380 mg, 44%) ^{1}H NMR (400 MHz, $CHCl_3$) δ7.30 (t, J = 7.3 Hz, 1H), 7.11 (t, J = 7.3 Hz, 1H), 6.68 (d, J = 7.3 Hz, 1H), 6.64 (d, J = 7.3 Hz, 1H), 4.24 (bs, 2H), 0.26 (s, 9H)

2-Ethynylaniline 43 [72]

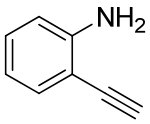

2-((trimethylsilyl)ethynyl)aniline **42** (380 mg, 2.0 mmol) was dissolved in 6 ml methanol and then 2 ml of 1 M aq. KOH solution was added. The reaction was stirred at room temperature for 2 h. The solvent was evaporated and subsequently the product was extracted with DCM. The DCM solution was dried with $NaSO_4$ and the solvent was removed in vacuo. The crude product was purified by column chromatography on silica (pentane/EtOAc 9:1) yielding 114 mg (49%) product. ^{1}H NMR (400 MHz, $CHCl_3$) δ7.34 (d, J = 7.3 Hz, 1H), 7.16 (t, J = 7.3 Hz, 1H), 6.69 (m, 2H), 4.25 (br s, 2H), 3.4 (s, 1H)

2-[(2-Aminophenyl)ethynyl]phenyl}methanol 46 [41]

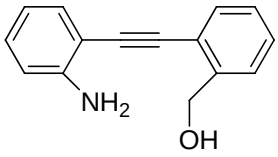

2-Iodobenzylalcohol **45** (4.0 g , 17 mmol), $Pd(PPh_3)_2Cl_2$ (239 mg, 0.34 mmol) and CuI (32 mg, 0.17 mmol) were added to a flame dried flask and put under N_2. Dry THF and dry triethylamine (3.8 ml, 27.4 mmol) were added. Subsequently the N_2 was replaced by H_2, the 2-ethynylaniline **43** was added and the solution was stirred for 4 h at room temperature. Then the mixture was diluted with DCM and washed with water. The water layers were extracted twice with DCM and the combined organic layers were washed twice with water and once with brine. The layers were dried over $MgSO_4$ and the solvent was removed under reduced pressure. The crude product was purified by column chromatography on silica with heptane/EtOAc 4:1, yielding the product as a white solid 2.6 g, 72%. ^{1}H NMR (400 MHz, $CHCl_3$) δ7.56 (dd, J = 7.3 Hz, 1H), 7.44 (dd, J = 7.3 Hz, 1H), 7.35 (m, 3H), 7.15 (ddt, J = 7.3 Hz, 1H), 6.72 (m, 2H), 4.89 (d, J = 6.2 Hz, 2H), 4.43 (br s, 2H), 1.99 (t, J = 6.3 Hz, 1H)

***tert*-Butyl(2-{[2-(hydroxymethyl)phenyl]ehynyl}phenyl)carbamate 47** [41]

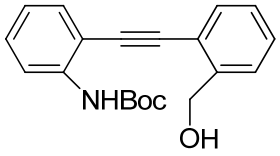

Compound **46** (2.6 g, 11.5 mmol) was dissolved in THF, subsequently bocanydride (2.77 g, 12.7 mmol) was added and the mixture was stirred in a sealed tube at 70°C for 2 days. The mixture was diluted with DCM and washed with a 10% citric acid solution once then twice with water and once with brine. The organic layer was dried with $MgSO_4$ and the solvent was removed *in vacuo* yielding the product as a white solid 3.6 g, 97%. ^{1}H NMR (400 MHz, $CHCl_3$) δ 8.14 (d, J = 7.4 Hz, 1H), 7.87 (s, 1H), 7.61 (dd, J = 7.3, 1.7 Hz, 1H), 7.45 (m, 2H), 7.34 (m, 3H), 7.01 (dt, J = 7.6, 1.1 Hz, 1H), 4.91 (d, J = 4.4 Hz, 2H), 2.50 (br s, 1H), 1.56 (s, 9H)

***tert*-Butyl(2-{(Z)-2-[2-(hydroxymethyl)phenyl]ehynyl}phenyl)carbamate 48** [41]

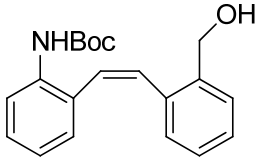

Compound **47** (3.6 g, 11.2 mmol) was dissolved in methanol, subsequently 10% Pd on barium sulfate (230 mg, 0.28 mmol Pd) and quinoline (332 µl, 2.8 mmol) were added to the mixture followed by stirring for 20 h. The mixture was filtered over celite and the solvent was removed. Column chromatography on silica with heptanes/EtOAc 4:1, yielded the product as a yellow solid 1.89 g, 54%. ^{1}H NMR (400 MHz, $CHCl_3$) δ 7.83 (br s, 1H), 7.31 (d, J = 7.3 Hz, 1H), 7.18 (m, 3H), 6.98 (m, 4H), 6.71 (br s, 1H), 7.65 (d, J = 12 Hz, 1H), 4.74 (d, J = 6.3 Hz, 1H), 1.41 (s, 9H)

***tert*-Butyl{2-[(Z)-2-(2-formylphenyl)ehynyl]phenyl}carbamate 49** [41]

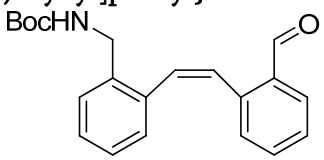

Compound **48** (1.89 g, 6.08 mmol) was dissolved in dry DCM and placed under N_2 in a flame dried flask. Subsequently Dess-Martin periodonate (3.1 g, 7.30 mmol) and $NaHCO_3$ (1.65 g, 19.7 mmol) were added to the mixture which was stirred for 80 min. The reaction was quenched with saturated aqueous Na_2SO_3 and the mixture was subsequently diluted with DCM. The layers were separated and the organic layer was washed with saturated aq. $NaHCO_3$ twice, once with water and once with brine. The organic layer was dried with $MgSO_4$ and the solvent was removed *in*

vacuo. Column chromatography on silica (heptanes/EtOAc 6:1) yielded the product as a yellow solid 1.83 g (93%). ^{1}H NMR (400 MHz, $CHCl_3$) δ10.23 (s, 1H), 7.88 (d, J = 8.3 Hz, 1H), 7.81 (dd, J = 7.6, 1.4 Hz, 1H), 7.35 (m, 2H), 7.17, (dt, J = 7.7, 1.7 Hz, 1H), 7.08 (d, J = 8.3 Hz, 1H), 6.99 (d, 7.7 Hz, 1H), 6.89 (t, J = 7.5 Hz, 1H), 6.78 (d, J = 11.9 Hz, 1H), 6.5 (br s, 1H), 1.43 (s, 9H)

5,6-Dihydrodibenzo[b,f]azocine 50 [41]

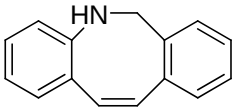

Compound **49** (1.73g, 5.38 mmol) was dissolved in 50 ml of a 2 M aq. HCl solution and stirred for 1 h. $NaBH_4$ (610 mg, 16.1 mmol) was then added to the solution and it was stirred for 20 h after which extra $NaBH_4$ (610 mg, 16.1 mmol) was added to the solution and it was stirred for an additional hour. The reaction was then quenched with water and the mixture was extracted twice with EtOAc and subsequently washed twice with 0.2 M aq. NaOH, water and brine. The organic layers were dried with $MgSO_4$ and the solvent was removed *in vacuo* yielding 1.1 g of product as a yellow solid (100% yield). ^{1}H NMR (400 MHz, $CHCl_3$) δ7.28-7.24 (m, 1H), 7.19 (m, 3H), 6.97 (dd, J = 7.8, 1.6 Hz, 1H), 6.88 (dt, J = 8.2, 1.5 Hz, 1H), 6.60 (dt, J = 8.2, 1.5 Hz, 1H), 6.54 (d, J = 12.8 Hz, 1H), 6.47 (d, J = 8.1 Hz, 1H), 6.36 (d, J = 12.8 Hz, 1H), 4.59 (s, 2H)

Methyl 5-dibenzo[b,f]azocin-f(6H)-yl-5-oxopentanoate 51

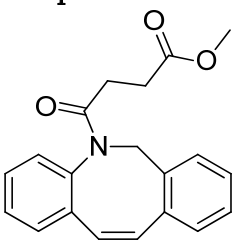

Compound **50** (1.11 g, 5.4 mmol) was dissolved in dry DCM and dry Et_3N (1.49 ml, 10.7 mmol). The solution was cooled to 0°C and subsequently succinyl chloride (1.17 ml, 8.1 mmol) was added to the mixture which was stirred for 1.5 h at 0 °C. The reaction was quenched by addition of water and the mixture was diluted with DCM. The organic layer was separated and washed twice with 2M aq. NaOH, 2M aq. HCl, water and once with brine. The organic layer was dried with $MgSO_4$ and the solvent was removed *in vacuo*. Column chromatography on silica (heptanes/EtOAc 1:2) yielded 1.18 g of the product as a yellow oil (60%). ^{1}H NMR (400 MHz, $CHCl_3$) δ 7.27-7.24 (m, 4H), 6.76 (d, J = 13.1 Hz, 1H), 6.61 (d, J = 13.1 Hz, 1H), 5.52 (d, J = 15.0 Hz, 1H), 4.25 (d, J = 15.0 Hz, 1H), 3.61 (s, 3H), 2.51 (m, 3H), 2.01 (m, 1H); ^{13}C NMR (100.59 MHz, $CDCl_3$): 177.4, 170.8, 140.5, 136.4, 135.8, 134.5, 132.6, 131.8, 130.8, 130.1, 128.5, 128.2, 128.0, 127.2, 126.9, 54.4, 51.6, 29.5, 29.0. HRMS (ESI+) (m/z) calculated for $C_{20}H_{19}NO_3$ $[M + Na]^+$ 344.12571, measured 344.12496.

Methyl 5-(11,12-dibromo-11,12-dihydrodibenzo[b,f]azocin-5(6H)-yl)-5-oxopentanoate 52

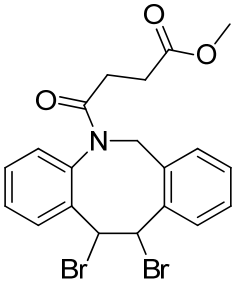

Compound **51** (1.19 g, 3.2 mmol) was dissolved in dry DCM and cooled to 0°C, subsequently Br_2 (0.17 ml, 3.2 mmol) was added and the resulting mixture was stirred for 50 min at 0 °C. The reaction was quenched with saturated aqueous Na_2SO_3 and the mixture diluted with DCM. The layers were separated and the organic layer was washed three times with aq. Na_2SO_3, two times with water and once with brine. The organic layer was dried with $MgSO_4$ and the solvent was evaporated under reduced pressure. Gradient column chromatography on silica (heptanes/EtOAc 3:1 → 2:1) yielded both isomers of the product as a white solid 1.54 g (100%). Analytical data of the major isomer are given. ^{1}H NMR (400 MHz, $CHCl_3$) δ 7.71 (d, J = 7.8 Hz, 1H), 7.19-7.00 (m, 5H), 6.78 (d, J = 7.6 Hz, 1H), 6.61 (d, J = 7.6 Hz, 1H), 5.92 (d, J = 9.9 Hz, 1H), 5.82 (d, J = 14.6 Hz, 1H), 5.51 (d, J = 7.6 Hz, 1H), 4.19 (d, J = 14.6 Hz, 1H), 3.61 (s, 3H), 2.95-2.35 (m, 3H), 2.13-1.92 (m, 1H); ^{13}C NMR (100.59 MHz, $CDCl_3$): 173.5, 172.0, 138.3, 137.0, 136.9, 132.8, 130.8, 130.7, 130.6, 129.6, 129.5, 128.9, 128.8, 128.6, 60.0, 55.5, 52.5, 51.7, 30.6, 29.2. HRMS (ESI+) (m/z) calculated for $C_{20}H_{19}Br_2NO_3$ $[M + Na]^+$ 503.96034, measured 503.96064.

Methyl 5-(11,12-didehydrodibenzo[b,f]azocin-5(6H)-yl)-5-oxopentanoate 39

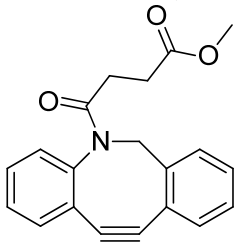

Compound **52** (1.6 g, 3.4 mmol) was added to a flame dried Schlenk and dissolved in dry THF. The mixture was cooled to -40°C. Subsequently KO^{t}Bu (6.7 ml of a 1 M solution in dry THF) was dropswise added after which the reaction mixture was stirred for 1.5 h when again KO^{t}Bu (1.7 ml) was added and stirred for a final 30 min at -40°C. Then the reaction mixture was poured into a large amount of water and extracted 3 times with DCM. The combined organic layers were washed three times with water and once with brine. The crude product was purified by gradient column chromatography on silica (heptanes/EtOAc 3:1 → 2:1) yielded 300 mg, 28% of the product as a light yellow oil. ^{1}H NMR (400 MHz, $CHCl_3$) δ 7.68 (d, J = 7.3 Hz, 1H), 7.49 (m, 1), 7.41-7.08 (m, 6H), 5.16 (d, J = 14.0 Hz, 1H), 3.62 (d, J = 14.0 Hz, 1H), 3.55 (s, 3H), 2.77-2.68 (m, 1H), 2.64-2.56 (m, 1H), 2.37-2.31 (m, 1H), 2.00-1.92 (m, 1H); ^{13}C NMR (100.59 MHz, $CDCl_3$): δ 173.3, 171.7, 151.4, 148.0, 132.3, 129.3, 128.8, 128.5, 128.1, 127.7, 127.1, 125.5, 123.1, 122.6, 114.9, 107.7, 55.4, 51.6, 29.6, 29.0 . HRMS (ESI+) (m/z) calculated for $C_{20}H_{17}NO_3$ $[M + Na]^+$ 342.11006, measured 342.11021.

3.3

General procedure for the kinetic studies of 39 with fluorinated compounds.

A stock solution of alkyne **39** (36 μmol/ml) and para-fluorobenzylazide **53** (36 μmol/ml) were prepared. Subsequently 250 μmol of each solution was taken and mixed in an NMR tube. Then the reaction was followed in time by ^{1}H NMR by measuring every 2 minutes.

methyl 4-(3-(4-fluorophenyl)-3H-dibenzo[b,f][1,2,3]triazolo[4,5-d]azocin-8(9H)-yl)-4-oxobutanoate 54

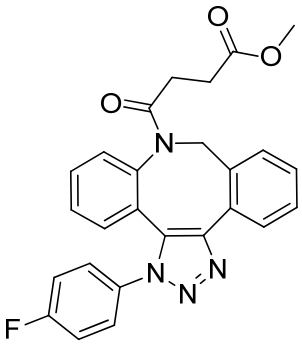

Compound **39** (80 mg, 0.25 mmol) was dissolved in DCM then 1-(azidomethyl)-4-fluorobenzene (57 mg, 0.38 mmol) was added to the mixture. The reaction mixture was stirred overnight. After evaporation of the solvent the crude product was purified by column chromatography on silica yielding 33 mg (30%) of the product as a white solid. ^{1}H NMR (400 MHz, $CHCl_3$) δ 7.73-7.67 (m, 1H), 7.49-7.44 (m, 2H), 7.42-7.38 (m, 1H), 7.31-7.24 (m, 1H), 7.17-7.24 (m, 2H), 7.10-6.93 (m, 5H), 5.99 (d, J = 16.9 Hz, 1H), 5.58 (s, 2H), 4.33 (d, J = 16.9 Hz, 1H), 3.6 (s, 3H), 2.44 (m, 1H), 2.23 (m, 1H), 2.09 (m, 1H), 1.80 (m, 1H). ^{13}C NMR (75 MHz, $CHCl_3$) δ173.2, 171.3, 163.7, 161.3, 143.1, 140.0, 135.9, 134.9, 131.8, 131.24, 130.68, 129.87, 129.62, 129.34, 129.12, 129.0, 127.9, 127.1, 124.3, 116.0, 115.8, 52.0, 51.6, 51.4, 29.2, 28.9;

Chapter 4:
4.1.1

3-nitro-7-diethylamino-coumarin 64 [76]

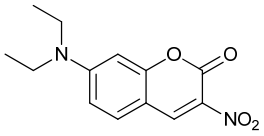

In a flame dried flask containing molecular sieves under a N_2-atmosphere, 4-diethyl-amino salicylaldehyde **62** (1.4g, 7.2 mmol) and ethylnitroacetate **63** (0.8 ml, 7.2 mmol) were dissolved in 20 ml n-butanol. Then 0.1 ml piperidine and 0.2 ml acetic acid were added and the mixture was refluxed for 26 h and subsequently cooled to rt. The reaction mixture was filtered and the solid was dissolved in hot DMF and filtered again to remove the mol sieves. Subsequently 100 ml of ice cold H_2O was added and a yellow solid crashed out of solution. Filtration yielded 1.17 g (4.45 mmol, 62%) of orange solid. ^{1}H NMR (400MHz, $CDCl_3$) δ 8.74 (s, 1H), 7.45 (d, J = 9.2 Hz, 1H), 6.71 (dd, J = 9.2, 2.2 Hz, 1H), 6.50 (d, J = 2.2 Hz, 1H), 3.50 (q, J = 7.3 Hz, 4H), 1.28 (t, J = 7.2 Hz, 6H).

3-amino-7-diethylamino-coumarin 65 [76]

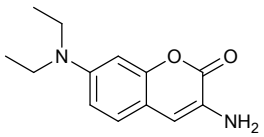

$SnCl_2$ was dissolved in conc. aq. HCl, then compound **64** (237 mg, 0.91 mmol) was slowly added to the solution over a period of 30 min, after which the reaction mixture was stirred for an additional 4 h. Subsequently the mixture was poured over 40 g of ice, put in an ice bath, and then NaOH was added until the solution was alkaline. The reaction mixture was filtered and subsequently

extracted with ether. The organic layers were washed with H_2O and dried over Na_2SO_4. Removal of the solvent yielded the product as a yellow solid (137 mg, 0.59 mmol, 65%). ^1H NMR (400MHz, $CDCl_3$) δ 7.11 (d, J = 8.8 Hz, 1H), 6.70 (s, 1H), 6.57 (m, 2H), 3.85 (br s, 2H), 3.38 (q, J = 7.1 Hz, 4H), 1.18 (t, J = 7.1 Hz, 6H).

3-azido-7-diethylamino-coumarin 61 [76]

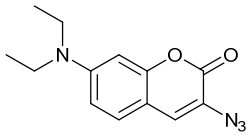

Compound **65** (100 mg, 0.43 mmol) was dissolved slowly in 10 ml of 17.2% aq. HCl, cooled to 0°C and then $NaNO_2$ (80.2 mg, 1.16 mmol) was added and the solution was stirred for 1 h at 0 °C. Subsequently $KOOCCH_3$ was added (2 g in 5 ml) until pH 4 was reached. NaN_3 (150 mg, 2.32 mmol) was added slowly to the mixture wich was then stirred for 5 h at 0 °C. The reaction mixture was then filtered and washed with ice cold H_2O, dissolved in ether and dried with Na_2SO_4. Evaporation of the solvent yielded 57.5 mg (0.22 mmol, 52%) of the product as a brown solid. ^1H NMR (400 MHz, $CDCl_3$) δ 7.19 (d, J = 8.8 Hz, 1H), 7.11 (s, 1H), 6.59 (dd, J = 8.8, 2.6 Hz, 1H), 6.51 (d, J = 2.6 Hz, 1H), 3.41 (q, J = 7.1 Hz, 4H), 1.21 (t, J = 7.1 Hz, 6H).

2.2'-O,O'-(1,1'-binaphtyl)-O,O'-dioxo-*N,N*-dimethylphospholidine 66

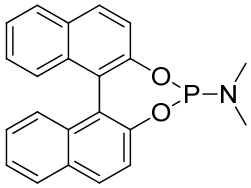

(*R,S*)-Binol (1.0 g, 3.5 mmol) was dissolved in 50 ml dry toluene under a nitrogen atmosphere. Subsequently 1 ml (5.5 mmol) hexamethylphosphortriamine was added to the solution and the reaction mixture was heated until reflux and stirred for 61 h. Evaporation of the solvent yielded the crude product as an oil which was recrystallized from $CHCl_3$ affording the pure product as a white solid (0.57g,1.58 mmol, 45%). ^1H NMR (400 MHz, $CDCl_3$) δ 2.75 (d, J = 9.20 Hz, 6H), 7.25-8.00 (m, 12H); ^{13}C NMR (95 MHz, $CDCl_3$) δ35.8 (d, J = 22.0 Hz), 121.8 (d, J = 1.0 Hz), 123.0 (d, J= 84.0 Hz), 124.9 (d. J = 18.1 Hz), 125.9, 126.8 (d, J = 6.0 Hz), 128.1 (d. J = 6.0 Hz.), 130.01 (d, J = 36.0 Hz), 130.8 (d, J = 47.4), 132.7 (d, J = 2.0 Hz), 149.51 (d, J = 38.3 Hz); ^{31}P NMR ($CDCI_3$): δ149.9.

Attempted synthesis of **7-(diethylamino)-3-(4-phenyl-1H-1,2,3-triazol-1-yl)-2H-chromen-2-one 69** [76]

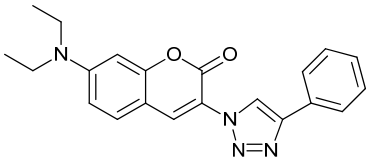

MonoPhos (0.5 mg, 2 µmol) was dissolved in 0.5 ml DMSO and added to a solution of $CuSO_4.5H_2O$ (0.85 mg, 2 µmol) in 1 ml H_2O the resulting solution was stirred for 15 min at rt. Compound **61** (50 mg, 0.19 mmol) and phenylacetylene (39 mg, 0.38 mmol) were placed in a round bottom flask and the Cu solution was added along with and 1.5 ml of H_2O. The reaction stirred for 3 h and samples

were taken periodically. The samples were extracted with $CDCl_3$, and analyzed by NMR. After 24 h there was still no product visible by ^1H NMR.

4.2.2

Attempted syntheses of **2-(6-azidohexyl)-9-(tridecan-7-yl)anthra[2,1,9-def:6,5,10-d'e'f']diisoquinoline-1,3,8,10(2H,9H)-tetraone 71***

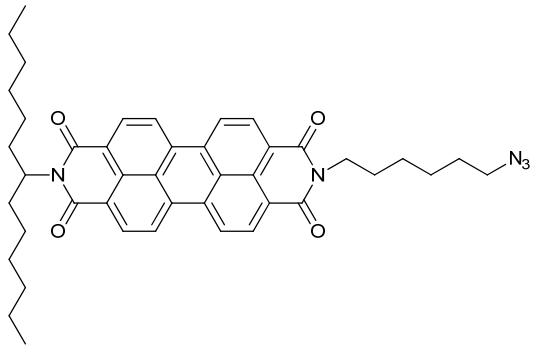

Method 1:
Compound **70** (100 mg, 0.136 mmol) was dissolved in 4 ml acetone and NaN_3 (13.3 mg, 0.204 mmol) was added to the solution. The mixture was stirred for 22 h after which the solvent was removed under reduced pressure. ^1H NMR showed only starting material and IR showed no evidence of an azide.

Method 2:
Compound **70** (25 mg, 34 µmol) was dissolved in 10 ml of THF and subsequently NaN_3 (11.5 mg, 170µmol) and Et_4NI (0.68 mg, 3.4µmol) dissolved in 10 ml H_2O were added to the solution. The reaction mixture was treated at reflux for 67 h. After allowing the reaction mixture to cool to rt the layers were separated, ^1H NMR/ IR of the organic layer showed that there was no product formed. The water layer was extracted with EtOAc, the EtOAc layer was dried and removed under reduced pressure. ^1H NMR and IR showed only starting material.

Method 3:
Compound **70** (25mg, 34 µmol) was dispersed in 5 ml DMF, then NaN_3 (2.4 mg, 37µmol) was added and the solution was stirred at 80 °C for 22 h. Subsequently 5 ml of H_2O was added to the mixture and the precipitated solid was filtrated and dried in vacuo at 60 °C for 1 h, yielding only starting material.

* Compound 71 contains an azide moiety, because azides are able to expel nitrogen to form a highly reactive nitrene. It is advised to be very careful and use a blast screen when working with azides.

2-(6-hydroxyhexyl)-9-(tridecan-7-yl)anthra[2,1,9-def:6,5,10-d'e'f']diisoquinoline-1,3,8,10(2H,9H)-tetraone 72

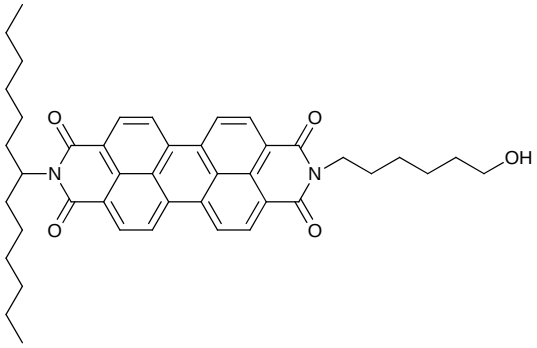

Compound **70** (50 mg, 68µmol) and AgOAc (11.5 mg, 68µmol) were dissolved in 5 ml glacial acetic acid and refluxed for 16h. After cooling to room temperature the mixture was filtrated and the solid was washed with DCM. To the filtrate 7.5 ml H_2O was added and the layers were separated. The water layer was extracted twice with DCM. The DCM layers were washed with cold H_2O four times. Then the solvent was removed and the remaining red solid, the crude acetate (^{1}H NMR (400 MHz, $CDCl_3$) δ8.63 (m, 8H), 5.19 (h, J = 5.8 Hz, 1H), 4.20 (t, J = 7.3 Hz, 2H), 4.07 (t, J = 6.4 Hz, 2H), 2.24 (m, 2H), 2.05 (s, 3H), 1.97-0.97 (m, 22H), 0.83(t, J = 6.9 Hz, 6H) was dissolved in 5 ml THF and 2.5 ml H_2O and 0.2 ml conc. HCl was added to the mixture which was then treated under reflux for 15 h. The THF was removed from the sample which was then diluted by 5 ml H_2O. The solution was extracted with DCM three times, washed three times with H_2O and dried with $MgSO_4$, after which the solvent was removed. Column chromatography on silica (eluent DCM) yielded 16.6 mg of alchol 7 as a red solid. ^{1}H NMR (400 MHz, $CDCl_3$) δ8.67 (m, 8H), 5.18 (h, J = 5.8 Hz, 1H), 4.22 (t, J = 7.3 Hz, 2H), 3.66 (t, J = 6.4 Hz, 2H), 2.24 (m, 2H), 2.11-1.05 (m, 22H), 0.82 (t, J = 6.8 Hz, 6H). ^{13}C NMR (95 MHz, $CDCl_3$) δ163.4, 163.3, 123.2, 123.1, 65.2, 63.0, 32.8, 32.6, 32.0, 29.5, 27.2, 25.5, 22.9, 14.3.

6-(1,3,8,10-tetraoxo-9-(tridecan-7-yl)-9,10-dihydroanthra[2,1,9-def:6,5,10-d'e'f']diisoquinolin-2(1H,3H,8H)-yl)hexyl 4-methylbenzenesulfonate 73

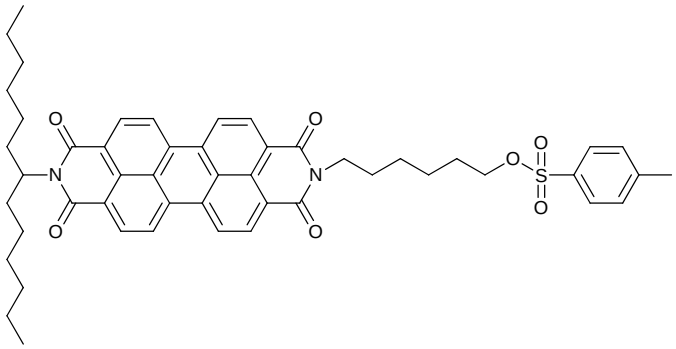

Compound **72** (40 mg, 74µmol) and p-toluenesulfonyl chloride (15 mg, 74µmol) were dissolved in 5 ml DCM and 0.1 ml pyridine. The solution was stirred for 4 d then it was quenched with 10 ml H_2O. The mixture was extracted three times with 10 ml DCM, the combined organic layers were washed with 5 ml H_2O and dried with $MgSO_4$ after which the solvent was evaporated. Column chromatography on silica (DCM/Acetone 10:1) yielded NMR quantities of the product as a red solid ^{1}H NMR (400 MHz, $CDCl_3$) δ8.60 (m, 8H), 7.63 (d, J = 8.1 Hz, 2H), 7.31 (d, J = 8.1 Hz, 2H),

5.19 (m, 1H), 4.21 (t, J = 7.3 Hz, 2H), 3.66 (t, J = 6.4 Hz, 2H), 2.96 (m, 4H), 2.43 (s, 3H), 2.25 (m, 2H), 1.95-1.09 (m, 18H), 0.84 (m, 6H).

3-amino-5-(fluorescein-thioureido)benzoic acid 75

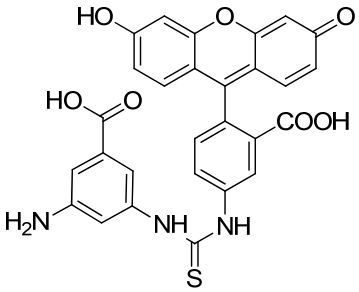

3,5-diaminobenzoic acid **73** (40 mg, 0.26 mmol) was dissolved in 10 ml methanol. To this solution a solution of fluorescein-5-isothiocyanate **74** (31.2 mg, 80 µmol) in 4 ml methanol was added, the resulting mixture was stirred for 28 h at rt. Gradient column chromatography on silica (pentane/EtOAc 5:1 to pentane/EtOAc 1:2) yielded 30 mg (56 µg, 70%) of the product as a dark yellow solid. ^{1}H NMR (300 MHz, CD_3OD) δ 8.10 (d, J = 8.6 Hz, 1H), 7.78 (dd, J = 8.2, 1.9 Hz, 1H), 7.27 (s, 1H), 7.20 (s, 2H), 7.13 (d, J = 8.2 Hz, 1H), 7.00 (s, 1H), 6.69-6.66 (m, 3H), 6.65 (s, 1H), 6.55 (dd, J = 8.7, 2.3 Hz, 2H); ^{13}C NMR (75 MHz, CD_3OD) δ 180.9, 170.2, 160.6, 153.1, 148.8, 148.3, 147.8, 141.3, 139.4, 139.3, 133.2, 131.7, 131.4, 129.9, 129.3, 129.1, 128.7, 127.9, 124.5, 120.2, 118.7, 114.8, 113.7, 113.3, 112.8, 110.4, 102.4; HRMS (ESI+) (m/z) calculated for $C_{28}H_{20}N_3O_7S^+$ $[M+H]^+$ 542.10165, measured 542.10370.

2,5-dioxopyrrolidin-1-yl pent-4-ynoate 78

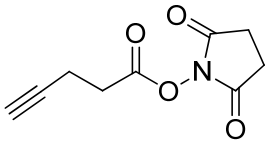

4-Pentynoic acid **76** (100 mg, 1.02 mmol) was dissolved in 10 ml dry DCM. Subsequently 1-ethyl-3-(3-dimethylaminopropyl)carbodiimide (215 mg, 1.12 mmol) and *N*-hydroxysuccinimide **77** (129 mg, 1.12 mmol) were added to the mixture, which was then stirred for 18 h at rt. Evaporation of the solvent yielded the crude product which was purified by column chromatography on silica (pentane/EtOAc 5:1 to pentane/EtOAc 2:1) yielding the product as 140 mg (0.72 mmol, 70%) of white solid. ^{1}H NMR (400 MHz, $CDCl_3$) δ2.93-2.79 (m, 7H), 2.67-2.57 (m, 2H), 2.05 (t, J = 2.1 Hz, 1H).

Attempted synthesis of **3-amino-5-(pent-4-ynamido)benzoic acid 79**

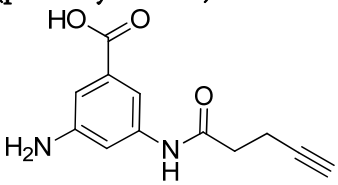

3,5-diaminobenzoic acid **73** (39 mg, 0.26 mmol) was dissolved in 5 ml DCM and DIPEA (93 µl, 0.56 mmol) was added to the solution. The mixture was cooled to 0°C and then the activated ester **78** (50 mg, 0.26 mmol) was slowly added to the solution. The reaction mixture was allowed to warm up to rt and stirred vigorously for 3 days. After evaporation of the solvent ^{1}H NMR showed only starting material.

8 References

[1] H. C. Kolb, M. G. Finn, K. B. Sharpless, *Angew. Chem., Int. Ed.* **2001**, *40*, 2004.

[2] V. V. Rostovtsev, L. G. Green, V. V. Fokin, K. B. Sharpless, *Angew. Chem., Int. Ed.* **2002**, *41*, 2596.

[3] C. W. Tornoe, C. Christensen, M. Meldal, *J. Org. Chem.* **2002**, *67*, 3057.

[4] R. Huisgen, G. Szeimies, L. Moebius, *Chem. Ber.* **1967**, *100*, 2494.

[5] J. C. Walsh, H. C. Kolb, *Chimia*, *64*, 29.

[6] N. G. Angelo, P. S. Arora, *J. Am. Chem. Soc.* **2005**, *127*, 17134.

[7] T. R. Chan, R. Hilgraf, K. B. Sharpless, V. V. Fokin, *Org. Lett.* **2004**, *6*, 2853.

[8] W. G. Lewis, F. G. Magallon, V. V. Fokin, M. G. Finn, *J. Am. Chem. Soc.* **2004**, *126*, 9152.

[9] V. O. Rodionov, S. I. Presolski, S. Gardinier, Y.-H. Lim, M. G. Finn, *J. Am. Chem. Soc.* **2007**, *129*, 12696.

[10] K. Tanaka, C. Kageyama, K. Fukase, *Tetrahedron Lett.* **2007**, *48*, 6475.

[11] F. Perez-Balderas, M. Ortega-Munoz, J. Morales-Sanfrutos, F. Hernandez-Mateo, F. G. Calvo-Flores, J. A. Calvo-Asin, J. Isac-Garcia, F. Santoyo-Gonzalez, *Org. Lett.* **2003**, *5*, 1951.

[12] J.-c. Meng, V. V. Fokin, M. G. Finn, *Tetrahedron Lett.* **2005**, *46*, 4543.

[13] S. Diez-Gonzalez, A. Correa, L. Cavallo, S. P. Nolan, *Chem.--Eur. J.* **2006**, *12*, 7558.

[14] L. S. Campbell-Verduyn, L. Mirfeizi, R. A. Dierckx, P. H. Elsinga, B. L. Feringa, *Chem. Commun.* **2009**, 2139.

[15] V. O. Rodionov, V. V. Fokin, M. G. Finn, *Angew. Chem., Int. Ed.* **2005**, *44*, 2210.

[16] F. Himo, T. Lovell, R. Hilgraf, V. V. Rostovtsev, L. Noodleman, K. B. Sharpless, V. V. Fokin, *J. Am. Chem. Soc.* **2005**, *127*, 210.

[17] H. Zheng, R. McDonald, D. G. Hall, *Chem. Eur. J.* **2010**, *16*, 5454.

[18] C. Nolte, P. Mayer, B. F. Straub, *Angew. Chem., Int. Ed.* **2007**, *46*, 2101.

[19] M. Meldal, C. W. Tornoe, *Chem. Rev.* **2008**, *108*, 2952.

[20] H. S. G. Beckmann, V. Wittmann, *Org. Lett.* **2007**, *9*, 1.

[21] L. S. Campbell-Verduyn, W. Szymanski, C. P. Postema, R. A. Dierckx, P. H. Elsinga, D. B. Janssen, B. L. Feringa, *Chem. Commun.* **2010**, *46*, 898.

[22] B. P. Duckworth, Y. Chen, J. W. Wollack, Y. Sham, J. D. Mueller, T. A. Taton, M. D. Distefano, *Angew. Chem., Int. Ed.* **2007**, *46*, 8819.

[23] B. P. Duckworth, Z. Zhang, A. Hosokawa, M. D. Distefano, *ChemBioChem* **2007**, *8*, 98.

[24] P. M. Clark, J. F. Dweck, D. E. Mason, C. R. Hart, S. B. Buck, E. C. Peters, B. J. Agnew, L. C. Hsieh-Wilson, *J. Am. Chem. Soc.* **2008**, *130*, 11576.

[25] C. Beyer, H.-A. Wagenknecht, *Chem. Commun.* **2010**, *46*, 2230.

[26] R. Varghese, H.-A. Wagenknecht, *Chem.--Eur. J.* **2009**, *15*, 9307.

[27] G. K. Wittig, Adolf, *Chem. Ber.* **1961**, *94*, 3260.

[28] N. J. Agard, J. A. Prescher, C. R. Bertozzi, *J. Am. Chem. Soc.* **2004**, *126*, 15046.

[29] N. J. Agard, J. M. Baskin, J. A. Prescher, A. Lo, C. R. Bertozzi, *Chem. Biol.* **2006**, *1*, 644.

[30] J. M. Baskin, J. A. Prescher, S. T. Laughlin, N. J. Agard, P. V. Chang, I. A. Miller, A. Lo, J. A. Codelli, C. R. Bertozzi, *Proc. Natl. Acad. Sci. U. S. A., Early Ed.* **2007**, 1.

[31] S. T. Laughlin, J. M. Baskin, S. L. Amacher, C. R. Bertozzi, *Science* **2008**, *320*, 664.

[32] P. V. Chang, J. A. Prescher, E. M. Sletten, J. M. Baskin, I. A. Miller, N. J. Agard, A. Lo, C. R. Bertozzi, *Proc. Natl. Acad. Sci. U. S. A.* **2010**, *107*, 1821.

[33] J. C. Jewett, C. R. Bertozzi, *Chem. Soc. Rev.* **2010**, *39*, 1272.

[34] E. M. Sletten, C. R. Bertozzi, *Org. Lett.* **2008**, *10*, 3097.

[35] F. C. A. De, B. D. Polizzotti, K. S. Anseth, *Nat. Mater.* **2009**, *8*, 659.

[36] C. Ornelas, J. Broichhagen, M. Weck, *J. Am. Chem. Soc.* **2010**, *132*, 3923.

[37] M. E. Martin, S. G. Parameswarappa, M. S. O'Dorisio, F. C. Pigge, M. K. Schultz, *Bioorg. Med. Chem. Lett.* **2010**, *20*, 4805.

[38] M. K. Schultz, S. G. Parameswarappa, F. C. Pigge, *Org. Lett.* **2010**, *12*, 2398.

[39] X. H. Ning, J. Guo, M. A. Wolfert, G. J. Boons, *Angew. Chem., Int. Ed.* **2008**, *47*, 2253.

[40] L. A. Canalle, S. S. van Berkel, L. T. de Haan, J. C. M. van Hest, *Adv. Funct. Mater.* **2009**, *19*, 3464.

[41] M. F. Debets, S. S. van Berkel, S. Schoffelen, F. Rutjes, J. C. M. van Hest, F. L. van Delft, *Chem. Commun.* **2010**, *46*, 97.

[42] E. M. Sletten, H. Nakamura, J. C. Jewett, C. R. Bertozzi, *J. Am. Chem. Soc.* **2010**, *132*, 11799.

[43] Y. Himeshima, T. Sonoda, H. Kobayashi, *Chem. Lett.* **1983**, 1211.

[44] L. Campbell-Verduyn, P. H. Elsinga, L. Mirfeizi, R. A. Dierckx, B. L. Feringa, *Org. Biomol. Chem.* **2008**, *6*, 3461.

[45] M. Clark, P. Kiser, *Polym. Int.* **2009**, *58*, 1190.

[46] B.-B. Ni, C. Wang, H. Wu, J. Pei, Y. Ma, *Chem. Commun.* **2010**, *46*, 782.

[47] Z. Li, T. S. Seo, J. Ju, *Tetrahedron Lett.* **2004**, *45*, 3143.

[48] F. Joliot, I. Curie, *Nature* **1934**, *133*, 201.

[49] M. E. Phelps, *Proc. Natl. Acad. Sci. U. S. A.* **2000**, *97*, 9226.

[50] R. Schirrmacher, C. Wangler, E. Schirrmacher, *Mini-Reviews in Organic Chemistry* **2007**, *4*, 317.

[51] D. W. Kim, D.-S. Ahn, Y.-H. Oh, S. Lee, H. S. Kil, S. J. Oh, S. J. Lee, J. S. Kim, J. S. Ryu, D. H. Moon, D. Y. Chi, *J. Am. Chem. Soc.* **2006**, *128*, 16394.

[52] O. Seung Jun, M. Christoph, C. Dae Yoon, K. Jung Young, K. Se Hun, R. Jin Sook, Y. Jeong Seok, M. Dae Hyuk, *Nucl. med. biol.* **2004**, *31*, 803.

[53] C. Thomas, D. Vijay, K. Ken, A. Angelo, M. Claude, J. R. Dahl, B. Abdelfatihe, M. Donald, Y. Archie, W. Shaoyin, T. Gilles, L. N. John, E. David, *Nucl. med. biol.* **1996**, *23*, 999.

[54] O. Seung Jun, C. Dae Yoon, M. Christoph, K. Jung Young, G. Hee Seop, K. Se Hun, R. Jin Sook, M. Dae Hyuk, *Nucl. med. biol.* **2005**, *32*, 899.

[55] J. Marik, J. L. Sutcliffe, *Tetrahedron Lett.* **2006**, *47*, 6681.

[56] U. Sirion, H. J. Kim, J. H. Lee, J. W. Seo, B. S. Lee, S. J. Lee, S. J. Oh, D. Y. Chi, *Tetrahedron Lett.* **2007**, *48*, 3953.

[57] M. Glaser, E. Aarstad, *Bioconjugate Chem.* **2007**, *18*, 989.

[58] Z.-B. Li, Z. Wu, K. Chen, F. T. Chin, X. Chen, *Bioconjugate Chem.* **2007**, *18*, 1987.

[59] S. H. Hausner, J. Marik, M. K. J. Gagnon, J. L. Sutcliffe, *J. Med. Chem.* **2008**, *51*, 5901.

[60] E. V. Anslyn, D. A. Dougherty, *Modern Physical Organic Chemistry*, University Science Books, United States of America, **2006**.

[61] Q. Wu, F. A. Merchant, K. R. Castleman, *Microscope image processing*, Elsevier/ Academic press, Amsterdam; Boston, **2008**.

[62] N. J. Emptage, *Curr. Opin. Pharmacol.* **2001**, *1*, 521.

[63] W. Denk, J. H. Strickler, W. W. Webb, *Science* **1990**, *248*, 73.

[64] M. Leopoldo, E. Lacivita, F. Berardi, R. Perrone, *Drug Discovery Today* **2009**, *14*, 706.

[65] L. E. Jennings, N. J. Long, *Chem. Commun.* **2009**, 3511.

[66] S. Lee, X. Chen, *Mol Imaging* **2009**, *8*, 87.

[67] R. H. Kimura, Z. Miao, Z. Cheng, S. S. Gambhir, J. R. Cochran, *Bioconjugate Chem.* **2010**, *21*, 436.

[68] R. O. Hynes, *Cell* **1992**, *69*, 11.

[69] M. E. Jung, A. B. Mossman, M. A. Lyster, *J. Org. Chem* **1978**, *43*, 3698.

[70] M. E. Jung, M. J. Martinelli, G. A. Olah, G. K. S. Prakash, J. Hu, in *e-ROS Encyclopedia of Reagents for Organic SYnthesis*, John Wiley & Sons, Ltd., **2001**, pp. 2845.

[71] M. E. Jung, S. J. Miller, *J. Am. Chem. Soc.* **1981**, *103*, 1984.

[72] N. Sakai, K. Annaka, A. Fujita, A. Sato, T. Konakahara, *J. Org. Chem.* **2008**, *73*, 4160.

[73] K. Sonogashira, Y. Tohda, N. Hagihara, *Tetrahedron Lett.* **1975**, 4467.

[74] J. Clayden, N. Greeves, S. Warren, P. Wothers, *Organic chemistry*, Oxford University Press, New York, **2001**.

[75] L. Kürti, B. Czakó, *stategic applications of named reactions in organic synthesis*, Elsevier inc., **2005**.

[76] K. Sivakumar, F. Xie, B. M. Cash, S. Long, H. N. Barnhill, Q. Wang, *Org. Lett.* **2004**, *6*, 4603.

[77] M.-S. Schiedel, C. A. Briehn, P. Bauerle, *Angew. Chem., Int. Ed.* **2001**, *40*, 4677.

[78] A. V. Ustinov, V. V. Dubnyakova, V. A. Korshun, *Tetrahedron* **2008**, *64*, 1467.

[79] H. Langhals, *Heterocycles* **1995**, *40*, 477.

[80] W.-C. Sun, K. R. Gee, D. H. Klaubert, R. P. Haugland, *J. Org. Chem.* **1997**, *62*, 6469.

[81] R. P. Haugland, *Handbook of Fluorescent Probes and Research Chemicals*, 6th ed., Molecular probes inc. , Eugene, **1996**.

[82] X.-M. Liu, H.-T. Lee, R. A. Reinhardt, L. A. Marky, D. Wang, *J. Controlled Release* **2007**, *122*, 54.